



This discussion paper is/has been under review for the journal Atmospheric Chemistry and Physics (ACP). Please refer to the corresponding final paper in ACP if available.

Ozone variability in the troposphere and the stratosphere from the first six years of IASI observations (2008–2013)

C. Wespes¹, P.-F. Coheur¹, L. K. Emmons², D. Hurtmans¹, S. Safieddine³,
C. Clerbaux^{1,3}, and D. P. Edwards²

¹Spectroscopie de l'Atmosphère, Service de Chimie Quantique et Photophysique, Université Libre de Bruxelles (U.L.B.), Brussels, Belgium

²National Center for Atmospheric Research, Boulder, CO, USA

³Sorbonne Universités, UPMC Univ. Paris 06; Université Versailles St-Quentin; CNRS/INSU, LATMOS-IPSL, Paris, France

Received: 14 August 2015 – Accepted: 19 September 2015 – Published: 14 October 2015

Correspondence to: C. Wespes (cwespes@ulb.ac.be) and P.-F. Coheur (pfcoheur@ulb.ac.be)

Published by Copernicus Publications on behalf of the European Geosciences Union.

Ozone variability in the troposphere and the stratosphere from the first six years of IASI observations

C. Wespes et al.

Title Page

Abstract

Introduction

Conclusions

References

Tables

Figures

◀

▶

◀

▶

Back

Close

Full Screen / Esc

Printer-friendly Version

Interactive Discussion



Abstract

In this paper, we assess how daily ozone (O_3) measurements from the Infrared Atmospheric Sounding Interferometer (IASI) on MetOp-A platform can contribute to the analyses of the processes driving O_3 variability in the troposphere and the stratosphere and, in the future, to the monitoring of long-term trends. The time development of O_3 during the first 6 years of IASI (2008–2013) operation is investigated with multivariate regressions separately in four different layers (ground–300, 300–150, 150–25, 25–3 hPa), by adjusting to the daily time series averaged in 20° zonal bands, seasonal and linear trend terms along with important geophysical drivers of O_3 variation (e.g. solar flux, quasi biennial oscillations). The regression model is shown to perform generally very well with a strong dominance of the annual harmonic terms and significant contributions from O_3 drivers, in particular in the equatorial region where the QBO and the solar flux contribution dominate. More particularly, despite the short period of IASI dataset available to now, two noticeable statistically significant apparent trends are inferred from the daily IASI measurements: a positive trend in the upper stratosphere (e.g. $1.74 \pm 0.77 \text{ DU yr}^{-1}$ between $30\text{--}50^\circ \text{ S}$) which is consistent with the turnaround for stratospheric O_3 recovery, and a negative trend in the troposphere at the mid-and high northern latitudes (e.g. $-0.26 \pm 0.11 \text{ DU yr}^{-1}$ between $30\text{--}50^\circ \text{ N}$), especially during summer and probably linked to the impact of decreasing ozone precursor emissions. The impact of the high temporal sampling of IASI on the uncertainty in the determination of O_3 trend has been further explored by performing multivariate regressions on IASI monthly averages and on ground-based FTIR measurements.

1 Introduction

Global climate change is one of the most important environmental problems of today and monitoring the behavior of the atmospheric constituents (radiatively active gases and those involved in their chemical production) is key to understand the present cli-

Ozone variability in the troposphere and the stratosphere from the first six years of IASI observations

C. Wespes et al.

Title Page

Abstract

Introduction

Conclusions

References

Tables

Figures

◀

▶

◀

▶

Back

Close

Full Screen / Esc

Printer-friendly Version

Interactive Discussion



Ozone variability in the troposphere and the stratosphere from the first six years of IASI observations

C. Wespes et al.

Title Page

Abstract

Introduction

Conclusions

References

Tables

Figures

◀

▶

◀

▶

Back

Close

Full Screen / Esc

Printer-friendly Version

Interactive Discussion



of precursors, long-range transport, stratosphere–troposphere – STE – exchanges), which are all strongly variable temporally and spatially (e.g. Logan et al., 2012; Hess and Zbinden, 2013; Neu et al., 2014). Overall, there are still today large differences in the value of the O_3 trends determined from independent studies and datasets in both the stratosphere and the troposphere (e.g. Oltmans et al., 1998, 2006; Randel and Wu, 2007; Gardiner et al., 2008; Vigouroux et al., 2008; Jiang et al., 2008; Kyrölä et al., 2010; Vigouroux et al., 2014). In order to improve on this and because O_3 has been recognized as an GCOS Essential Climate Variables (ECVs), the scientific community has underlined the need of acquiring high quality global, long-term and homogenized ozone profile records from satellites (Randel and Wu, 2007; Jones et al., 2009; WMO, 2007, 2011, 2014). This specifically has resulted in the ESA Ozone Climate Change Initiative (O_3 -CCI; <http://www.esa-ozone-cci.org/>).

The Infrared Atmospheric Sounding Interferometer (IASI) onboard the polar orbiting MetOp, with its unprecedented spatiotemporal sampling of the globe, its high radiometric stability and the long duration of its program (3 successive instruments to cover 15 years) provides in principle an excellent means to contribute to the analyses of the O_3 variability and trends. This is further strengthened by the possibility to discriminate well with IASI, the O_3 distributions and variability in the troposphere and the stratosphere, as shown in earlier studies (Boynard et al., 2009; Wespes et al., 2009, 2012; Dufour et al., 2010; Barret et al., 2011; Scannell et al., 2012; Safieddine et al., 2013). Here, we use the first 6 years (2008–2013) of the new O_3 dataset provided by IASI on MetOp-A to perform a first analysis of the O_3 time development in the stratosphere and in the troposphere. This is achieved globally by using zonal averages in 20° latitude bands and a multivariate linear regression model which accounts for various natural cycles affecting O_3 . We also explore in this paper to which extent the exceptional temporal sampling of IASI can counterbalance the short period of data available for assessing trends in partial columns.

In Sect. 2, we give a short description of IASI and of the O_3 retrieved columns used here. Section 3 details the multivariate regression model used for fitting the time series.

Ozone variability in the troposphere and the stratosphere from the first six years of IASI observations

C. Wespes et al.

Title Page

Abstract

Introduction

Conclusions

References

Tables

Figures

◀

▶

◀

▶

Back

Close

Full Screen / Esc

Printer-friendly Version

Interactive Discussion

lite observations (Anton et al., 2011; Dufour et al., 2012; Gazeaux et al., 2012; Parrington et al., 2012; Pommier et al., 2012; Scannell et al., 2012; Oetjen et al., 2014). Generally, the results show good agreements between FORLI-O₃ and independent measurements with a low bias (< 10%) in the total column and in the vertical profile, except in UTLS where a positive bias of 10–15% is reported (Dufour et al., 2012; Gazeaux et al., 2012; Oetjen et al., 2014).

In this study, only daytime O₃ IASI observations from good spectral fits (RMS of the spectral residual lower than $3.5 \times 10^{-8} \text{ W}/(\text{cm}^2 \text{ sr cm}^{-1})$) have been analyzed. Daytime IASI observations are characterized by a better vertical sensitivity to the troposphere associated with a higher surface temperature and a higher thermal contrast (Clerbaux et al., 2009; Boynard et al., 2009). Furthermore, cloud contaminated scenes with cloud cover < 13% (Hurtmans et al., 2012) were removed using cloud information from the Eumetcast operational processing (August et al., 2012).

An example of typical FORLI-O₃ averaging kernel functions for one mid-latitude observation in July (45° N/66° E) is represented on Fig. 1. The layers have been defined as: ground–300 hPa (MLT), 300–150 hPa (UTLS), 150–25 hPa (MLS) and above 25 hPa (US), so that they are characterized by a DOFS (Degrees Of Freedom for Signal) close to 1 with a maximum sensitivity approximatively in the middle of the layers, except for the 300–150 hPa layer which has a reduced sensitivity. Taken globally, the DOFS for the entire profile ranges from ~ 2.5 in cold polar regions to ~ 4.5 in hot tropical regions, depending mostly on surface temperature, with a maximum sensitivity in the upper troposphere and in the lower stratosphere (Hurtmans et al., 2012). In the MLT, a maximum of sensitivity peaks around 6–8 km altitude for almost all situations (Wespes et al., 2012). Figure 2 presents July 2010 global maps of averaged FORLI-O₃ partial columns for two partial layers (MLT and MLS), and of the associated DOFS and a priori contribution (calculated as $X_a - \mathbf{A} \times X_a$, where X_a is the a priori profile and \mathbf{A} , the averaging kernel matrix, following the formalism of Rodgers, 2000). The two layers exhibit different sensitivity patterns: in the MLT, the DOFS typically range from 0.4 in the cold polar regions to 1 in regions characterized by high thermal contrast with

medium humidity, such as the mid-latitude continental Northern Hemisphere (N.H.) (Clerbaux et al., 2009). Lower DOFS values in the intertropical belt are explained by an overlapping from water vapor lines. In contrast, the DOFS for the MLS are globally almost constant and close to one, with only slightly lower values (0.9) over polar regions. The a priori contribution is anti-correlated with the sensitivity, as expected. It ranges between a few % to $\sim 30\%$ and does not exceed 20% on 20° zonal averages in the troposphere (see Supplement; Fig. S3, dashed lines), while the a priori contribution is smaller than $\sim 12\%$ in the middle stratosphere. These findings indicate that the IASI MLS time series should accurately represent stratospheric variations, while the time series in the troposphere may reflect to some extent variations from the upper layers in addition to the real variability in the troposphere. In order to quantify this effect, the contribution of the stratosphere in the tropospheric ozone as seen by IASI has been estimated with a global 3-D chemical transport model (MOZART-4). We show that it varies between 30 and 60% depending on latitude and season. Details of the model-observation comparisons can be found in the Supplement (see Figs. S2 and S3). The fact that IASI MLT O_3 is “contaminated” to a significant extend with variations in stratospheric O_3 should be kept in mind when analyzing IASI MLT O_3 .

3 Fitting method

3.1 Statistical model

In order to characterize the changes in ozone measured by IASI and to allow separation of trend due to ODS from trend due to other processes, we use a multiple linear regression model accounting for a linear trend and for variations related to dynamical processes and solar flux. More specifically, the time series analysis is based on the

Ozone variability in the troposphere and the stratosphere from the first six years of IASI observations

C. Wespes et al.

Title Page

Abstract

Introduction

Conclusions

References

Tables

Figures

◀

▶

◀

▶

Back

Close

Full Screen / Esc

Printer-friendly Version

Interactive Discussion



fitting of daily (or monthly) median partial columns in different latitude band following:

$$O_3(t) = Cst + x_1 \cdot \text{trend} + \sum_{n=1,2} [a_n \cdot \cos(n\omega t) + b_n \cdot \sin(n\omega t)] + \sum_{j=2}^m x_j X_{\text{norm},j}(t) + \varepsilon(t) \quad (1)$$

where t is the number of days (or months), x_1 is the 6 year trend coefficient in the data, $\omega = 2\pi/365.25$ for the daily model (or $2\pi/12$ for the monthly model) and $X_{\text{norm},j}$ are independent geophysical variables, the so-called “explanatory variables” or “proxies”, which are in this study normalized over the period of IASI observation (2008–2013), as:

$$X_{\text{norm}}(t) = 2(X(t) - X_{\text{median}}) / (X_{\text{max}} - X_{\text{min}}) \quad (2)$$

$\varepsilon(t)$ in Eq. (1) represents the residual variation which is not described by the model and which is assumed to be autoregressive with time lag of 1 day (or 1 month). The constant term (Cst) and the coefficients a_n , b_n , x_j are estimated by the least-squares method and their standard errors are calculated from the covariance matrix of the coefficient estimates and corrected to take into account the uncertainty due to the autocorrelation of the noise residual. The median is used as a statistical average since it is more adequate against the outliers than the normal mean (Kyrölä et al., 2006, 2010). Note that, similarly to Kyrölä et al. (2010), the model has been applied on O_3 mixing ratios rather than on partial columns but without significant improvement on the fitting residuals and R values.

3.2 Geophysical variables

In Eq. (1), harmonic time series with period of a year and a half year are used to account for the Brewer–Dobson circulation and the solar insolation (a_1 and b_1 coefficients), and for the meridional circulation (a_2 and b_2 coefficients), respectively (Kyrölä et al., 2010), all of these effects being of a periodic nature, while geophysical variables

Ozone variability in the troposphere and the stratosphere from the first six years of IASI observations

C. Wespes et al.

Title Page

Abstract

Introduction

Conclusions

References

Tables

Figures

◀

▶

◀

▶

Back

Close

Full Screen / Esc

Printer-friendly Version

Interactive Discussion



Ozone variability in the troposphere and the stratosphere from the first six years of IASI observations

C. Wespes et al.

Title Page

Abstract

Introduction

Conclusions

References

Tables

Figures

◀

▶

◀

▶

Back

Close

Full Screen / Esc

Printer-friendly Version

Interactive Discussion

(X_j) are used here to parameterize the ozone variations on non-seasonal timescales. The chosen proxies are $F_{10.7}$, QBO¹⁰, QBO³⁰, ENSO, NAO/AAO, the first three being the most commonly used (“standard”) proxies to describe the natural ozone variability, i.e. the solar radio flux at 10.7 cm and the quasi-biennial oscillation (QBO) which is represented by two orthogonal zonal components of the equatorial stratospheric wind measured at 10 and 30 hPa, respectively (e.g. Randel and Wu, 2007). The three other proxies, ENSO, NAO and AAO, are used to account for other important fluctuating dynamical features: the El Niño/Southern Oscillation, the North Atlantic Oscillation and the Antarctic Oscillation, respectively. Table 1 lists the selected proxies, their sources and their resolutions. The time series of these proxies normalized over the 2000–2013 period following Eq. (2) are shown in Fig. 3a and b and they are shortly described hereafter:

- *Solar flux*: over the period 2008–2013, the radio solar flux increases from about 65 units in 2008 to 180 units in 2013 and is characterized by a specific daily “fingerprint” (see Fig. 3a). Note that because the period of IASI observations do not cover a full 11 year solar cycle, it could affect the determination of the trend in the regression procedure. The difficulty in discriminating both components is a known problem for such multivariate regression: it feeds into their uncertainties and it can lead to biases in the coefficients determination (e.g. Soukharev et al., 2006).
- *QBO terms*: the QBO of the equatorial winds is a main component of the dynamics of the tropical stratosphere (Chipperfield et al., 1994, 2003; Randel and Wu, 1996, 2007; Logan et al., 2003; Tian et al., 2006; Fadnavis and Beig, 2009; Hauchecorne et al., 2010). It strongly influences the distributions of stratospheric O₃ propagating alternatively westerly and easterly with a mean period of 28 to 29 months. Positive and negative vertical gradients alternate periodically. At the top of the vertical QBO domain, predominance of easterlies, while, at the bottom, westerly winds are more frequent. For accounting for the out-of-phase re-

account in the model in the harmonic and the linear trend terms of the Eq. (1) (e.g. Logan et al., 2012). Including harmonic terms having 4 and 3 month periods in the model has been tested to describe O_3 dependency on shorter scales (e.g. Gebhardt et al., 2014), but this did not improved the results in terms of residuals and uncertainty of correlation coefficients.

3.3 Iterative backward variable selection

Similarly to previous studies (e.g. Steinbrecht et al., 2004; Mäder et al., 2007, 2010; Knibbe et al., 2014), we perform an iterative stepwise backward elimination approach, based on p values of the regression coefficients for the rejection, to select the most relevant combination of the above described regression variables (harmonic, linear and explanatory) to fit the observations. The minimum p value for a regression term to be removed (exit tolerance) is set at 0.05, which corresponds to a significance of 95%. The initial model which includes all regression variables is fitted first. Then, at each iteration, the variables characterized by p values larger than 5 % are rejected. At the end of the iterative process, the remaining terms are considered to have significant influence on the measured O_3 variability while the rejected variables are considered to be non-significant. The correction accounting for the autocorrelation in the noise residual is then applied to give more confidence in the coefficients determination.

4 Ozone variations observed by IASI

In this section, we first examine the ozone variations in IASI time series during 2008–2013 in the four layers defined in the troposphere and the stratosphere to match the IASI sensitivity (Sect. 2). The regression coefficients determined from the multiple linear procedure (Sect. 3) are analyzed in Sect. 4.2. The ability of IASI to derive apparent trends is examined in Sect. 4.3.

Ozone variability in the troposphere and the stratosphere from the first six years of IASI observations

C. Wespes et al.

Title Page

Abstract

Introduction

Conclusions

References

Tables

Figures

◀

▶

◀

▶

Back

Close

Full Screen / Esc

Printer-friendly Version

Interactive Discussion



4.1 O₃ time series from IASI

Figure 4a shows the time development of daily O₃ number density over the entire altitude range of the retrieved profiles based on daily medians. The time series cover the six years of available IASI observations and are separated in three 20° latitude belts: 30–50° N (top panel), 10–10° S (middle panel) and 30–50° S (bottom panel). The figure shows the well-known seasonal cycle at mid-latitudes in the troposphere and the stratosphere with maxima observed in spring-summer and in winter-spring, respectively, and a strong stability of ozone layers with time in the equatorial belt. At high latitudes of both hemispheres, the high ozone concentrations and the large amplitude of the seasonal cycle observed in LS and UTLS are mainly the consequence of the large-scale downward poleward Brewer–Dobson circulation which is prominent in later winter below 25 km.

Figure 4b presents the estimated statistical uncertainty on the O₃ profiles retrieved from FORLI. This total error depends on the latitude and the season, reflecting, amongst other, the influence of signal intensity, of interfering water lines and of thermal contrast under certain conditions (e.g. temperature inversion, high thermal contrast at the surface). It usually ranges between 10 and 30 % in the troposphere and in the UTLS (Upper Troposphere–Lower Stratosphere), except in the equatorial belt due to the low O₃ amounts (see Fig. 4a) which leads to larger relative errors. The retrieval errors are usually less than 5 % in the stratosphere.

The relative variability (given as the standard deviation) of the daily median O₃ time series presented in Fig. 4a is shown in Fig. 5, as a function of time and altitude. It is worth noting that, except in the UTLS over the equatorial band, the standard deviation is larger than the estimated retrieval errors of the FORLI-O₃ data (~ 25 vs. ~ 15 % and ~ 10 vs. ~ 5 %, on average over the troposphere and the stratosphere, respectively), reflecting that the high natural temporal variability of O₃ in zonal bands is well captured with FORLI (Dufour et al., 2012; Hurtmans et al., 2012). The standard deviation is larger in the troposphere and in the stratosphere below 20 km where dynamic processes

Ozone variability in the troposphere and the stratosphere from the first six years of IASI observations

C. Wespes et al.

Title Page

Abstract

Introduction

Conclusions

References

Tables

Figures

◀

▶

◀

▶

Back

Close

Full Screen / Esc

Printer-friendly Version

Interactive Discussion



Ozone variability in the troposphere and the stratosphere from the first six years of IASI observations

C. Wespes et al.

Title Page

Abstract

Introduction

Conclusions

References

Tables

Figures

◀

▶

◀

▶

Back

Close

Full Screen / Esc

Printer-friendly Version

Interactive Discussion



play an important role. The largest values ($> 70\%$ principally in the northern latitudes during winter) are measured around 9–15 km altitude. They highlight the influence of tropopause height variations and the STE processes. In the stratosphere, the variability is always lower than 20 % and becomes negligible in the equatorial region. Interestingly, the lowest troposphere of the N.H. (below 700 hPa; < 4 km) is marked by an increase in both O_3 concentrations (Fig. 4a) and standard deviations (between ~ 30 and $\sim 45\%$) in spring-summer. This likely indicates a photochemical production of O_3 associated with anthropogenic precursor emissions (e.g. Logan et al., 1985; Dufour et al., 2010; Safieddine et al., 2013).

The zonal representation of the O_3 variability seen by IASI is given in Fig. 6. It shows the daily number density at altitude levels corresponding to maximum of sensitivity in the four analyzed layers in most of the cases (600 hPa – ~ 6 km; 240 hPa – ~ 10 km; 80 hPa – ~ 20 km; 6 hPa – ~ 35 km) (Sect. 2). The top panel (~ 35 km) reflects well the photochemical O_3 production by sunlight with the highest values in the equatorial belt during the summer ($\sim 3 \times 10^{12}$ molecules cm^{-3}). The middle panels (~ 20 and ~ 10 km) shows the transport of ozone rich-air to high latitudes in late winter (up to $\sim 6 \times 10^{12}$ molecules cm^{-3} in the N.H.) which is induced by the Brewer–Dobson circulation. The fact that the patterns are similar in ~ 10 km mainly reflects the low sensitivity of IASI to that level compared to the others. Finally, the lower panel (~ 6 km) presents high O_3 levels in spring at high latitudes ($\sim 1.4 \times 10^{12}$ molecules cm^{-3} in the N.H.), which likely reflects both the STE processes and the contribution from the stratosphere due to the medium IASI sensitivity to that layer (cfr. Sect. 2 and Supplement), and a shift from high to middle latitudes in summer which could be attributed to anthropogenic O_3 production. The MLT panel also reflects the seasonal oscillation of the Inter-Tropical Convergence Zone (ITCZ) around the Equator and the large fire activity in spring around 20–40° S.

Ozone variability in the troposphere and the stratosphere from the first six years of IASI observations

C. Wespes et al.

Title Page

Abstract

Introduction

Conclusions

References

Tables

Figures

◀

▶

◀

▶

Back

Close

Full Screen / Esc

Printer-friendly Version

Interactive Discussion



to the averaged O_3 values. The largest amplitude in the annual cycle is found in the N.H. between 30 and 50° N where O_3 peaks in July after the highest solar elevation (in June) following a progressive buildup during spring-summer. In agreement with FTIR observations (e.g. Steinbrecht et al., 2006; Vigouroux et al., 2008), a shift of the O_3 maximum from spring (March–April) to late summer (August–September) is found as one moves from high to low latitudes in the N.H. In the S.H., the general shape of the annual cycle which shows a peak in October–November before the highest solar elevation (in December), results from loss mechanisms depending on annual cycle of temperatures and other trace gases. Other effects such as changing Brewer–Dobson circulation, light absorption and tropical stratopause oscillations may also considerably impact on the cycle in this layer (Brasseur and Solomon, 1984; Schneider et al., 2005).

2. In the lower stratosphere (MLS and UTLS, middle panels), the pronounced amplitudes of the annual cycle is dominated by the influence of the Brewer Dobson circulation with the highest O_3 values observed over polar regions (reaching $\sim 6 \times 10^{18}$ molecules cm^{-2} on average vs. $\sim 2 \times 10^{18}$ molecules cm^{-2} on average in the equatorial belt). The maximum is shifted from late winter at high latitudes to spring at lower latitudes.
3. In MLT (bottom panel), we clearly see a large hemispheric difference with the highest values over the N.H. (also in UTLS). Maxima are observed in spring, reflecting more effective STE processes. A particularly broad maximum from spring to late summer is observed in the 30–50° N band. It probably points to anthropogenic production of O_3 . This has been further investigated in the Supplement through MOZART4-IASI comparison by using constant anthropogenic emissions in the model settings (see Fig. S1). The results show clear differences between the modeled and the observed MLT seasonal cycles, which highlights the need for further investigation of the role of anthropogenically produced O_3 and the realism of anthropogenic emissions inventories.

Ozone variability in the troposphere and the stratosphere from the first six years of IASI observations

C. Wespes et al.

Title Page

Abstract

Introduction

Conclusions

References

Tables

Figures



Back

Close

Full Screen / Esc

Printer-friendly Version

Interactive Discussion

circulation (cfr. Fig. 6 and Fig. 7) and the sign of the coefficient accounts for the winter-spring maxima in both hemispheres (negative values in the S.H. and positive ones in the N.H). In the US, they vary only slightly (around -5 to 5%) and account for the weak summer maximum.

2. The QBO and solar flux proxies are generally minor (scaled coefficients $< 10\%$) and they are even statistically non-significant contributors to O_3 variations after accounting for the autocorrelation in the noise residual, except for the UTLS in equatorial region (scaled coefficients of 10 – 15%) where they are important drivers of O_3 variations (e.g. Logan et al., 2003; Steinbrecht et al., 2006b; Soukharev and Hood, 2006; Fadnavis and Beig, 2009) Previous studies have indeed supported the solar influence on the lower stratospheric equatorial dynamics (e.g. Soukharev and Hood, 2006; McCormack et al., 2007). Note that the QBO³⁰ proxy (data not shown) has negative coefficients for the mid-latitudes, which is in line with Frossard et al. (2013).

3. The contributions described by the ENSO and NAO/AAO proxies are generally very weak, with scaled coefficients lower than 5% , and, in many cases, even not statistically significant when taking into account the correlation in the noise residuals. Despite of this, it is worth pointing out that their effects to the O_3 variations are in agreement with previous studies, which have shown large regions of negative coefficients for NAO North of $40^\circ N$, and large regions of positive and negative coefficient estimates for ENSO, North of $30^\circ N$ and South of $30^\circ S$, respectively (Rieder et al., 2013; Frossard et al., 2013).

Finally, we see in Fig. 8b, large uncertainties associated with the regression coefficients in UTLS in comparison with other layers, and in polar regions in comparisons with other bands. We interpret this as an effect from the high natural variability of O_3 measured by IASI in UTLS (see Fig. 5) and from missing parameterizations and low temporal sampling of daytime IASI measurements over the poles, respectively.

4.3 Multivariate regression results: trend over 2008–2013

An additional goal of the multivariate regression method applied to the IASI O₃ time series is to determine the annual trend term and its associated uncertainty. Despite the fact that more than 10 years of observations, corresponding to the large scale of solar cycle, is usually required to perform such a trend analysis, we could argue that statistically relevant trends could possibly be derived from the first six years of IASI observations, owing to the high spatio-temporal frequency (daily) of IASI global observations, to the daily “fingerprint” in the solar flux (see Fig. 3a), possibly making it distinguishable from a linear trend, and to its weak contribution to O₃ variations (see Sect. 4.2 and references therein). To verify the specific advantage of IASI in terms of frequency sampling, we compare, in the subsections below, the statistical relevance of the trends when retrieved from the monthly averaged IASI datasets vs. the daily averages as above, in the 20° zonal bands.

4.3.1 Regressions applied on daily vs. monthly averages

Figure 9 (top) provides, as an example for the 30–50° S latitude band, the 6 year time series of the IASI O₃ partial column in the US (dark blue), for daily averages (left panels) vs monthly averages (right panels), along with the results from the regression procedure (light blue). Note that either daily or monthly F10.7, NAO and AAO proxies (see Table 1) are used depending on the frequency of the IASI O₃ averages to be adjusted. The middle panels provide the deseasonalised IASI and fitted time series as well as the residuals (red curves). The fitted signal in DU of each proxy is shown on the bottom panels. The O₃ time series and the solar flux signal resulting from the adjustment without the linear term trend in the regression model are also represented (orange lines in middle and bottom panels, respectively). When it is not included in the regression model, the linear trend term is not compensated by the solar flux term in the daily averages, which leads to larger residuals (80 % without vs. 44 % with the linear term), while it is largely compensated by the solar flux term in the monthly averages (75 % with-

Ozone variability in the troposphere and the stratosphere from the first six years of IASI observations

C. Wespes et al.

Title Page

Abstract

Introduction

Conclusions

References

Tables

Figures



Back

Close

Full Screen / Esc

Printer-friendly Version

Interactive Discussion



Ozone variability in the troposphere and the stratosphere from the first six years of IASI observations

C. Wespes et al.

Title Page

Abstract

Introduction

Conclusions

References

Tables

Figures

◀

▶

◀

▶

Back

Close

Full Screen / Esc

Printer-friendly Version

Interactive Discussion



out vs. 60 % with the linear term). In this example, the linear and solar flux terms are even not simultaneously retained in the iterative stepwise backward procedure when applied on the monthly averages while they are when applied on daily averages. This effective co-linearity of the linear and the monthly solar flux terms translates to a large uncertainty for the trend coefficient in monthly data and leads, in this example, to a not statistically significant linear term of $1.21 \pm 1.30 \text{ DU yr}^{-1}$ when derived from monthly averages vs. a significant trend of $1.74 \pm 0.77 \text{ DU yr}^{-1}$ from daily averages.

This brings us to the important conclusion that, thanks to the unprecedented sampling of IASI, apparent trends can be detected in FORLI-O₃ time series even on a short period of measurements. This supports the need for regular and high frequency measurements for observing ozone variations underlined in other studies (e.g. Saunois et al., 2012). The O₃ trends from the daily averages of IASI measurements are discussed and compared with results from the monthly averages in the subsection below.

4.3.2 O₃ trends from daily averages

Table 2 summarizes the trends and their uncertainties in the 95 % confidence limit, calculated for each 20° zonal band and for the 4 partial and the total columns. For the sake of comparison, the trends are reported for both the daily (top values) and the monthly (bottom values) averages, and their uncertainties account for the auto-correlation in the noise residuals considering a time lag of 1 day or 1 month, respectively. We show that the daily and monthly trends fall within each other uncertainties but that the trends in monthly averages are shown to be mostly non-significant in comparison with those from daily averages for the reasons discussed above (Sect. 4.3.1). Table 3 summarizes the trends in the daily averages for two 3 month periods: June–July–August (JJA) and December–January–February (DJF).

From Tables 2 and 3, we observe very different trends according to the latitude and the altitude. From Table 2, we find for the total columns that the trends derived from the daily medians are only significant at high northern latitudes and that they are interestingly of the same order as those obtained from other satellites and assimilated satellite

Ozone variability in the troposphere and the stratosphere from the first six years of IASI observations

C. Wespes et al.

Title Page

Abstract

Introduction

Conclusions

References

Tables

Figures

◀

▶

◀

▶

Back

Close

Full Screen / Esc

Printer-friendly Version

Interactive Discussion



trends in winter. A non-significant trend is also calculated for the 70–90° S band in spring (data not shown). This could indicate the strong influence of changing stratospheric temperatures on ozone depletion from year to year (e.g. Dhomse et al., 2006), leading to larger uncertainties in our trends estimations and larger fitting residuals (see Sect. 4.2) due to the fact that the stratospheric temperature is not taken into account as an explanatory variable in the model.

2. In the MLS, one can see that, except in the high latitude bands, the trends are either non-significant or significantly negative. This is in agreement with the trend analysis of Jones et al. (2009) for the 20–25 km altitude range over the 1997–2008 period, as well as with other studies at N.H. latitudes, which investigated O₃ changes in the 18–25 km range between 1996 and 2005 (Miller et al., 2006; Yang et al., 2006; Kivi et al., 2007). The results derived separately for summer and winter in Table 3 are also in line with those of Kivi et al. (2007) which reported contrasted trends in the Arctic MLS depending on season.
3. In the UTLS, negative trends are calculated in the tropics and significant positive trends are found in the mid- and high latitudes of N.H., these latter falling within the uncertainties of those reported by Kivi et al. (2007) for the tropopause–150 hPa layer between 1996 and 2003. The large positive trends calculated at Northern latitudes (e.g. 1.28 ± 0.82 DU year⁻¹ in the 70–90° N band) contribute for ~ 30 % to the positive trend for the total column. This result is in agreement with Yang et al. (2006) which reported that UTLS contributes 50 % to positive trends for the total columns measured in the mid-latitudes of the N.H. from ozonesondes. In that study, these positive trends were linked to changes in atmospheric dynamics either related to natural variability induced by potential vorticity and tropopause height variations or related to anthropogenic climate change. Hence, the apparent increase in total ozone in the mid-latitudes of the N.H. seen by IASI would reflect the combined contribution of dynamical variability and declining ozone-depleting substances (e.g. Weatherhead and Andersen, 2006; WMO, 2006; Harris et al.,

Ozone variability in the troposphere and the stratosphere from the first six years of IASI observations

C. Wespes et al.

Title Page

Abstract

Introduction

Conclusions

References

Tables

Figures

◀

▶

◀

▶

Back

Close

Full Screen / Esc

Printer-friendly Version

Interactive Discussion



2008; Nair et al., 2014). It is worth to keep in mind that these effects are not independently accounted for in the regression model. Previous studies reported, however, that dynamical and chemical processes are physically coupled in the atmosphere, making difficult to define unambiguously such drivers in a statistical model (e.g. Mäder et al., 2007; Harris et al., 2008). On a seasonal basis (see Table 3), the trends seen by IASI at Northern latitudes in summer are all significantly positive and increasing towards the pole. Note that the trends in upper layers may contribute to the ones calculated in UTLS due to the medium IASI sensitivity to that layer (cfr. Sect. 2).

4. In the MLT, most of the trends are significantly negative (Tables 2 and 3). The non-significant trends in polar regions could be partly related to the lack of IASI sensitivity to tropospheric O₃ (see Sect. 2, Fig. 2). On a seasonal basis, we see that the negative trends are more pronounced during the JJA period (around $-0.25 \pm 0.10 \text{ DU yr}^{-1}$) for all bands except between 30° N and 10° S. In the N.H., these results tend to confirm the leveling off of tropospheric ozone observed in recent years during the summer months (Logan et al., 2012). This trend, however, remains difficult to interpret because it could be linked to a variety of processes including most importantly: the decline of anthropogenic emissions of ozone precursors, the increase of UV-induced O₃ destruction in the troposphere and STE processes (Isaksen et al., 2005; Logan et al., 2012; Parrish et al., 2012; Hess and Zbinden, 2013). As for the upper layers, our results for the Arctic are in agreement with the findings of Kivi et al. (2007) which reported an increase of ozone in the ground-400 hPa layer in summer over the 1996–2003 period following changes in the Arctic Oscillation. It is also worth to keep in mind that due to medium sensitivity of IASI to the troposphere, ozone variations in upper layers may largely impact on the trends seen by IASI in that layer (cfr. Sect. 2 and Supplement).

4.3.3 O₃ trends from IASI vs. FTIR data

In order to validate the trends inferred from IASI in the US and in the total columns, we compare them with those obtained from ground-based FTIR measurements at several NDACC stations (Network for the Detection of Atmospheric Composition Change, available at http://www.ndsc.ncep.noaa.gov/data/data_tbl/) by using the same fitting procedure and taking into account the autocorrelation in the noise residuals. A box of $1^\circ \times 1^\circ$ centered on the stations has been used for the collocation criterion. The regression model is applied on the daily FTIR data for a series of time periods starting after the turnaround point (from 1998 for mid-latitude stations and from 2000 for polar stations), as well as for the same periods as recently studied in Vigouroux et al. (2014) for the sake of comparison. Note that because we are not interested here in validating the IASI columns which was achieved in previous papers (e.g. Dufour et al., 2014; Oetjen et al., 2014) but in validating the trends obtained from IASI, we did not correct biases between IASI and FTIR due to different vertical sensitivity and a priori information. The results are given in DU year⁻¹ in Table 4. We see large significant positive total column trends from IASI at middle and polar stations (e.g. 5.26 ± 4.72 DU yr⁻¹ at Ny-Alesund), especially during spring and which are in agreement with the trends reported in Knibbe et al. (2014) for the 2001–2010 period. This trend is not obtained from the FTIR data for which trends are found to be mostly non-significant (even not retained in the stepwise elimination procedure in some cases) as reported in Vigouroux et al. (2014), except at Jungfraujoch which shows a trend of 5.28 ± 4.82 DU yr⁻¹ over the 2008–2012 period. For the periods starting before 2000, we calculated from FTIR, in agreement with Vigouroux et al. (2014), a significantly negative trend at Ny-Alesund for the total column and significantly positive trends at polar stations for the US. In addition, we see from Table 4 a leveling off of O₃ at polar stations in the US after 2003, as previously reported in Vigouroux et al. (2014), which was explained by a compensation effect between the decrease of solar cycle after its maximum in 2001–2002 and a positive trend. These

Ozone variability in the troposphere and the stratosphere from the first six years of IASI observations

C. Wespes et al.

Title Page

Abstract

Introduction

Conclusions

References

Tables

Figures

◀

▶

◀

▶

Back

Close

Full Screen / Esc

Printer-friendly Version

Interactive Discussion



trends are, however, non-significant and inferred only from few FTIR measurements (see Number of days column, Table 4).

From IASI, it is worth to point out that, in all cases, positive trends are calculated in the US (even if some are not significant) and that these trends are consistent with those calculated from FTIR data covering a ~ 11 year period and starting after the turnaround (e.g. at Thule; $1.24 \pm 1.09 \text{ DU yr}^{-1}$ from IASI for the period 2008–2013 vs. $1.42 \pm 0.78 \text{ DU yr}^{-1}$ from the FTIR over 2001–2012). This is illustrated for three stations (Ny-Alesund, Thule and Kiruna) in Fig. 10 which compares the time series from IASI (2008–2013, in red) with those from FTIR covering periods starting after the turnaround (in blue). Their associated trends as well as the trend calculated from FTIR covering the IASI period (in green) are also indicated.

The results obtained for trends inferred from IASI vs. FTIR tend to confirm the conclusion drawn in Sects. 4.3.1 and 4.3.2, that the temporal sampling of IASI provides good confidence in the determination of the trends even on periods shorter than those usually required from other observational means.

5 Summary and conclusions

In this study, we have analyzed 6 years of IASI O_3 profile measurements as well as the total O_3 columns based on the profile. Four layers have been defined following the ability of IASI to provide reasonably independent information on the ozone partial columns: the mid-lower troposphere (MLT), the upper troposphere – lower stratosphere (UTLS), the mid-lower stratosphere (MLS) and the upper stratosphere (US). Based on daily values of these four partial or of the total columns in 20° zonal averages, we have demonstrated the capability of IASI for capturing large scale ozone variability (seasonal cycles and trends) in these different layers. We have presented daytime vertical and latitudinal distributions for O_3 as well as their evolution with time and we have examined the underlying dynamical or chemical processes. The distributions were found to be controlled by photochemical production leading to a maximum in summer

Ozone variability in the troposphere and the stratosphere from the first six years of IASI observations

C. Wespes et al.

Title Page

Abstract

Introduction

Conclusions

References

Tables

Figures

◀

▶

◀

▶

Back

Close

Full Screen / Esc

Printer-friendly Version

Interactive Discussion



Ozone variability in the troposphere and the stratosphere from the first six years of IASI observations

C. Wespes et al.

Title Page

Abstract

Introduction

Conclusions

References

Tables

Figures

◀

▶

◀

▶

Back

Close

Full Screen / Esc

Printer-friendly Version

Interactive Discussion



at equatorial region in the US, while they reflect the impact of the Brewer–Dobson circulation with maximum in winter-spring at mid- and high latitude in the MLS and in the troposphere. The effect of the photochemical production of O₃ from anthropogenic precursor emissions was also observed in the troposphere with a shift in the timing of the maximum from spring to summer in the mid-latitudes of the N.H.

The dynamical and chemical contributions contained in the daily time development of IASI O₃ have been analyzed by fitting the time series in each layer and for the total column with a set of parameterized geophysical variables, a constant factor and a linear trend term. The model was shown to perform well in term of residuals (< 10 %), correlation coefficients (between 0.70 and 0.99) and statistical uncertainties (< 7 %) for each fitted proxies. The annual harmonic terms (seasonal behavior) were found to be largely dominant in all layers but the US, with fitted amplitudes decreasing from high to low latitudes in agreement with the Brewer–Dobson circulation. The QBO and solar flux terms were calculated to be important only in the equatorial region, while other dynamical proxies accounted for in the regression (ENSO, NAO, AAO) were found negligible.

Despite the short time period of available IASI dataset used in this study (2008–2013) and the potential ambiguity between the solar and the linear trend terms, statistically significant trends were derived from the six first years of daily O₃ partial columns measurements (on the contrary to monthly averages which lead to mostly non-significant trends). This result which was strengthened from comparisons with the regression applied on local FTIR measurements, is remarkable as it demonstrates the added value of IASI exceptional frequency sampling for monitoring medium to long-term changes in global ozone concentrations. We found two important apparent trends:

1. Significant positive trends in the upper stratosphere, especially at high latitudes in both hemispheres (e.g. $1.74 \pm 0.77 \text{ DU yr}^{-1}$ in the 30–50° S band), which is consistent with a probable “turnaround” for upper stratospheric O₃ recovery (even if the causes of such a turnaround are still under investigations). In addition, the

References

- Andersen, S. B. and Knudsen, B. M.: The influence of polar vortex ozone depletion on NH mid-latitude ozone trends in spring, *Atmos. Chem. Phys.*, 6, 2837–2845, doi:10.5194/acp-6-2837-2006, 2006.
- 5 Andersen, S. B., Weatherhead, E. C., Stevermer, A., Austin, J., Brühl, C., Fleming, E. L., de Grandpré, J., Grewe, V., Isaksen, I., Pitari, G., Portmann, R. W., Rognerud, B., Rosenfield, J. E., Smyshlyaev, S., Nagashima, T., Velders, G. J. M., Weisenstein, D. K., and Xia, K.: Comparison of recent modeled and observed trends in total column ozone, *J. Geophys. Res.*, 111, D02303, doi:10.1029/2005JD006091, 2006.
- 10 Anton, M., Loyola, D., Clerbaux, C., Lopez, M., Vilaplana, J., Banon, M., Hadji-Lazaro, J., Valks, P., Hao, N., Zimmer, W., Coheur, P., Hurtmans, D., and Alados-Arboledas, L.: Validation of the Metop-A total ozone data from GOME-2 and IASI using reference ground-based measurements at the Iberian peninsula, *Remote Sens. Environ.*, 115, 1380–1386, 2011.
- August, T., Klaes, D., Schlüssel, P., Hultberg, T., Crapeau, M., Arriaga, A., O’Carroll, A., Cop-
15 pens, D., Munro, R., and Calbet, X.: IASI on Metop-A: operational Level 2 retrievals after five years in orbit, *J. Quant. Spectrosc. Ra.*, 114, 1340–1371, 2012.
- Barret, B., Le Flochmoen, E., Sauvage, B., Pavelin, E., Matricardi, M., and Cammas, J. P.: The detection of post-monsoon tropospheric ozone variability over south Asia using IASI data, *Atmos. Chem. Phys.*, 11, 9533–9548, doi:10.5194/acp-11-9533-2011, 2011.
- 20 Bourassa, A. E., Degenstein, D. A., Randel, W. J., Zawodny, J. M., Kyrölä, E., McLinden, C. A., Sioris, C. E., and Roth, C. Z.: Trends in stratospheric ozone derived from merged SAGE II and Odin-OSIRIS satellite observations, *Atmos. Chem. Phys.*, 14, 6983–6994, doi:10.5194/acp-14-6983-2014, 2014.
- Boynard, A., Clerbaux, C., Coheur, P.-F., Hurtmans, D., Turquety, S., George, M., Hadji-
25 Lazaro, J., Keim, C., and Meyer-Arnek, J.: Measurements of total and tropospheric ozone from IASI: comparison with correlative satellite, ground-based and ozonesonde observations, *Atmos. Chem. Phys.*, 9, 6255–6271, doi:10.5194/acp-9-6255-2009, 2009.
- Brasseur, G. and Solomon, S.: *Aeronomy of the Middle Atmosphere*, edited by: Reidel, D., Publishing Company, Dordrecht, the Netherlands, 441 pp., 1984.
- 30 Brohede, S., McLinden, C. A., Urban, J., Haley, C. S., Jonsson, A. I., and Murtagh, D.: Odin stratospheric proxy NO_y measurements and climatology, *Atmos. Chem. Phys.*, 8, 5731–5754, doi:10.5194/acp-8-5731-2008, 2008.

Ozone variability in the troposphere and the stratosphere from the first six years of IASI observations

C. Wespes et al.

Title Page

Abstract

Introduction

Conclusions

References

Tables

Figures

◀

▶

◀

▶

Back

Close

Full Screen / Esc

Printer-friendly Version

Interactive Discussion



Ozone variability in the troposphere and the stratosphere from the first six years of IASI observations

C. Wespes et al.

Title Page

Abstract

Introduction

Conclusions

References

Tables

Figures

◀

▶

◀

▶

Back

Close

Full Screen / Esc

Printer-friendly Version

Interactive Discussion



Chipperfield, M. P.: A three-dimensional model study of long-term mid-high latitude lower stratosphere ozone changes, *Atmos. Chem. Phys.*, 3, 1253–1265, doi:10.5194/acp-3-1253-2003, 2003.

Chipperfield, M. P., Kinnersley, J. S., and Zawodny, J.: A two-dimensional model study of the QBO signal in SAGE II NO₂ and O₃, *Geophys. Res. Lett.*, 21, 589–592, 1994.

Clarisse, L., Hurtmans, D., Clerbaux, C., Hadji-Lazaro, J., Ngadi, Y., and Coheur, P.-F.: Retrieval of sulphur dioxide from the infrared atmospheric sounding interferometer (IASI), *Atmos. Meas. Tech.*, 5, 581–594, doi:10.5194/amt-5-581-2012, 2012.

Clerbaux, C. and Crevoisier, C.: New Directions: infrared remote sensing of the troposphere from satellite: less, but better, *Atmos. Environ.*, 72, 24–26, 2013.

Clerbaux, C., Boynard, A., Clarisse, L., George, M., Hadji-Lazaro, J., Herbin, H., Hurtmans, D., Pommier, M., Razavi, A., Turquety, S., Wespes, C., and Coheur, P.-F.: Monitoring of atmospheric composition using the thermal infrared IASI/MetOp sounder, *Atmos. Chem. Phys.*, 9, 6041–6054, doi:10.5194/acp-9-6041-2009, 2009.

Coheur, P.-F., Barret, B., Turquety, S., Hurtmans, D., Hadji-Lazaro, J., and Clerbaux, C.: Retrieval and characterization of ozone vertical profiles from a thermal infrared nadir sounder, *J. Geophys. Res.*, 110, D24, doi:10.1029/2005JD005845, 2005.

Crevoisier, C., Clerbaux, C., Guidard, V., Phulpin, T., Armante, R., Barret, B., Camy-Peyret, C., Chaboureaud, J.-P., Coheur, P.-F., Crépeau, L., Dufour, G., Labonnote, L., Lavanant, L., Hadji-Lazaro, J., Herbin, H., Jacquinet-Husson, N., Payan, S., Péquignot, E., Pierangelo, C., Sellitto, P., and Stubenrauch, C.: Towards IASI-New Generation (IASI-NG): impact of improved spectral resolution and radiometric noise on the retrieval of thermodynamic, chemistry and climate variables, *Atmos. Meas. Tech.*, 7, 4367–4385, doi:10.5194/amt-7-4367-2014, 2014.

de Laat, A. T. J., van der A, R. J., and van Weele, M.: Tracing the second stage of ozone recovery in the Antarctic ozone-hole with a "big data" approach to multivariate regressions, *Atmos. Chem. Phys.*, 15, 79–97, doi:10.5194/acp-15-79-2015, 2015.

Dhomse, S., Weber, M., Wohltmann, I., Rex, M., and Burrows, J. P.: On the possible causes of recent increases in northern hemispheric total ozone from a statistical analysis of satellite data from 1979 to 2003, *Atmos. Chem. Phys.*, 6, 1165–1180, doi:10.5194/acp-6-1165-2006, 2006.

Dufour, G., Eremenko, M., Orphal, J., and Flaud, J.-M.: IASI observations of seasonal and day-to-day variations of tropospheric ozone over three highly populated areas of China: Beijing,

Ozone variability in the troposphere and the stratosphere from the first six years of IASI observations

C. Wespes et al.

Title Page

Abstract

Introduction

Conclusions

References

Tables

Figures

◀

▶

◀

▶

Back

Close

Full Screen / Esc

Printer-friendly Version

Interactive Discussion

Shanghai, and Hong Kong, Atmos. Chem. Phys., 10, 3787–3801, doi:10.5194/acp-10-3787-2010, 2010.

Dufour, G., Eremenko, M., Griesfeller, A., Barret, B., LeFlochmoën, E., Clerbaux, C., Hadji-Lazaro, J., Coheur, P.-F., and Hurtmans, D.: Validation of three different scientific ozone products retrieved from IASI spectra using ozonesondes, Atmos. Meas. Tech., 5, 611–630, doi:10.5194/amt-5-611-2012, 2012.

Fadnavis, S. and Beig, J.: Quasibiennial oscillation in ozone and temperature over tropics, J. Atmos. Solar Terr. Phys., 71, 1450–1455, doi:10.1016/j.jastp.2008.11.012, 2009.

Frossard, L., Rieder, H. E., Ribatet, M., Staehelin, J., Maeder, J. A., Di Rocco, S., Davison, A. C., and Peter, T.: On the relationship between total ozone and atmospheric dynamics and chemistry at mid-latitudes – Part 1: Statistical models and spatial fingerprints of atmospheric dynamics and chemistry, Atmos. Chem. Phys., 13, 147–164, doi:10.5194/acp-13-147-2013, 2013.

Gardiner, T., Forbes, A., de Mazière, M., Vigouroux, C., Mahieu, E., Demoulin, P., Velazco, V., Notholt, J., Blumenstock, T., Hase, F., Kramer, I., Sussmann, R., Stremme, W., Mellqvist, J., Strandberg, A., Ellingsen, K., and Gauss, M.: Trend analysis of greenhouse gases over Europe measured by a network of ground-based remote FTIR instruments, Atmos. Chem. Phys., 8, 6719–6727, doi:10.5194/acp-8-6719-2008, 2008.

Gazeaux, J., Clerbaux, C., George, M., Hadji-Lazaro, J., Kuttippurath, J., Coheur, P.-F., Hurtmans, D., Deshler, T., Kovilakam, M., Campbell, P., Guidard, V., Rabier, F., and Thépaut, J.-N.: Intercomparison of polar ozone profiles by IASI/MetOp sounder with 2010 Concordiasi ozonesonde observations, Atmos. Meas. Tech., 6, 613–620, doi:10.5194/amt-6-613-2013, 2013.

Hadjinicolaou, P., Pyle, J. A., and Harris, N. R. P.: The recent turnaround in stratospheric ozone over northern middle latitudes: a dynamical modeling perspective, Geophys. Res. Lett., 32, L12821, doi:10.1029/2005GL022476, 2005.

Harris, N. R. P., Kyrö, E., Staehelin, J., Brunner, D., Andersen, S.-B., Godin-Beekmann, S., Dhomse, S., Hadjinicolaou, P., Hansen, G., Isaksen, I., Jrrar, A., Karpetchko, A., Kivi, R., Knudsen, B., Krizan, P., Lastovicka, J., Maeder, J., Orsolini, Y., Pyle, J. A., Rex, M., Vanicek, K., Weber, M., Wohltmann, I., Zanis, P., and Zerefos, C.: Ozone trends at northern mid- and high latitudes – a European perspective, Ann. Geophys., 26, 1207–1220, doi:10.5194/angeo-26-1207-2008, 2008.

Ozone variability in the troposphere and the stratosphere from the first six years of IASI observations

C. Wespes et al.

Title Page

Abstract

Introduction

Conclusions

References

Tables

Figures

◀

▶

◀

▶

Back

Close

Full Screen / Esc

Printer-friendly Version

Interactive Discussion



Hauchecorne, A., Bertaux, J. L., Dalaudier, F., Keckhut, P., Lemennais, P., Bekki, S., Marchand, M., Lebrun, J. C., Kyrölä, E., Tamminen, J., Sofieva, V., Fussen, D., Vanhellemont, F., Fanton d'Andon, O., Barrot, G., Blanot, L., Fehr, T., and Saavedra de Miguel, L.: Response of tropical stratospheric O₃, NO₂ and NO₃ to the equatorial Quasi-Biennial Oscillation and to temperature as seen from GOMOS/ENVISAT, *Atmos. Chem. Phys. Discuss.*, 10, 9153–9171, doi:10.5194/acpd-10-9153-2010, 2010.

Hess, P. G. and Zbinden, R.: Stratospheric impact on tropospheric ozone variability and trends: 1990–2009, *Atmos. Chem. Phys.*, 13, 649–674, doi:10.5194/acp-13-649-2013, 2013.

Hofmann, D. J.: Recovery of Antarctic ozone hole, *Nature*, 384, 222–223, doi:10.1038/384222a0, 1996.

Hood, L. L. and Soukharev, B. E.: Solar induced variations of odd nitrogen: multiple regression analysis of UARS HALOE data, *Geophys. Res. Lett.*, 33, L22805, doi:10.1029/2006GL028122, 2006.

Hurtmans, D., Coheur, P., Wespes, C., Clarisse, L., Scharf, O., Clerbaux, C., Hadji-Lazaro, J., George, M., and Turquety, S.: FORLI radiative transfer and retrieval code for IASI, *J. Quant. Spectrosc. Ra.*, 113, 1391–1408, 2012.

Isaksen, I. S. A., Zerefos, C. S., Kourtidis, K., Meleti, C., Dalsøren, S. B., Sundet, J. K., Grini, A., Zanis, P., and Balis, D.: Tropospheric ozone changes at unpolluted and semipolluted regions induced by stratospheric ozone changes, *J. Geophys. Res.*, 110, D02302, doi:10.1029/2004JD004618, 2005.

Jiang, X., Pawson, S., Camp, C. D., Nielsen, E., Shia, R., Liao, T., Jeev, K., Limpasuvan, V., and Yung, Y. L.: Interannual variability and trends in extratropical ozone, Part II: Southern Hemisphere, *J. Atmos. Sci.*, 65, 3030–3041, 2008.

Jones, A., Urban, J., Murtagh, D. P., Eriksson, P., Brohede, S., Haley, C., Degenstein, D., Bourassa, A., von Savigny, C., Sonkaew, T., Rozanov, A., Bovensmann, H., and Burrows, J.: Evolution of stratospheric ozone and water vapour time series studied with satellite measurements, *Atmos. Chem. Phys.*, 9, 6055–6075, doi:10.5194/acp-9-6055-2009, 2009.

Kivi, R., Kyrö, E., Turunen, T., Harris, N. R. P., von der Gathen, P., Rex, M., Andersen, S. B., and Wohltmann, I.: Ozone-sonde observations in the Arctic during 1989–2003: ozone variability and trends in the lower stratosphere and free troposphere, *J. Geophys. Res.*, 112, D08306, doi:10.1029/2006JD007271, 2007.

Ozone variability in the troposphere and the stratosphere from the first six years of IASI observations

C. Wespes et al.

Title Page

Abstract

Introduction

Conclusions

References

Tables

Figures

◀

▶

◀

▶

Back

Close

Full Screen / Esc

Printer-friendly Version

Interactive Discussion



Logan, J. A., Jones, D. B. A., Megretskaia, I. A., Oltmans, S. J., Johnson, B. J., Vömel, H., Randel, W. J., Kimani, W., and Schmidlin, F. J.: Quasi-biennial oscillation in tropical ozone as revealed by ozonesonde and satellite data, *J. Geophys. Res.*, 108, 4244, doi:10.1029/2002JD002170, 2003.

5 Logan, J. A., Staehelin, J., Megretskaia, I. A., Cammas, J.-P., Thouret, V., Claude, H., De Backer, H., Steinbacher, M., Scheel, H.-E., Stübi, R., Fröhlich, M., and Derwent, R.: Changes in ozone over Europe: analysis of ozone measurements from sondes, regular aircraft (MOZAIC) and alpine surface sites, *J. Geophys. Res.*, 117, D09301, doi:10.1029/2011JD016952, 2012.

10 Mäder, J. A., Staehelin, J., Brunner, D., Stahel, W. A., Wohltmann, I., and Peter, T.: Statistical modelling of total ozone: selection of appropriate explanatory variables, *J. Geophys. Res.*, 112, D11108, doi:10.1029/2006JD007694, 2007.

Mäder, J. A., Staehelin, J., Peter, T., Brunner, D., Rieder, H. E., and Stahel, W. A.: Evidence for the effectiveness of the Montreal Protocol to protect the ozone layer, *Atmos. Chem. Phys.*, 10, 12161–12171, doi:10.5194/acp-10-12161-2010, 2010.

15 Manney, G. L., Santee, M. L., Froidevaux, L., Hoppel, K., Livesey, N. J., and Waters, J. W.: EOS MLS observations of ozone loss in the 2004–2005 Arctic winter, *Geophys. Res. Lett.*, 33, L04802, doi:10.1029/2005GL024494, 2006.

20 Manney, G., Santee, M. L., Rex, M., Livesey, N. J., Pitts, M. C., Veefkind, P., Nash, E. N., Wohltmann, I., Lehmann, R., Froidevaux, L., Poole, L. R., Schoeberl, M. R., Haffner, D. P., Davies, J., Dorokhov, V., Gernandt, H., Johnson, B., Kivi, R., Kyrö, E., Larsen, N., Levelt, P. F., Makshitas, A., McElroy, C. T., Nakajima, H., Parrondo, M. C., Tarasick, D. W., von der Gathen, P., Walker, K. A., and Zinoviev, N. S.: Unprecedented Arctic ozone loss in 2011, *Nature*, 478, 469–475, doi:10.1038/nature10556, 2011.

25 McCormack, J. P., Siskind, D. E., and Hood, L. L.: Solar-QBO interaction and its impact on stratospheric ozone in a zonally averaged photochemical transport model of the middle atmosphere, *J. Geophys. Res.*, 112, D16109, doi:10.1029/2006JD008369, 2007.

McLinden, C. A., Tegtmeier, S., and Fioletov, V.: Technical Note: A SAGE-corrected SBUV zonal-mean ozone data set, *Atmos. Chem. Phys.*, 9, 7963–7972, doi:10.5194/acp-9-7963-2009, 2009.

30 Miller, A. J., Cai, A., Tiao, G., Wuebbles, D. J., Flynn, L. E., Yang, S.-K., Weatherhead, E. C., Fioletov, V., Petropavlovskikh, I., Meng, X.-L., Guillas, S., Nagatani, R. M., and Reinsel, G. C.:

Ozone variability in the troposphere and the stratosphere from the first six years of IASI observations

C. Wespes et al.

[Title Page](#)[Abstract](#)[Introduction](#)[Conclusions](#)[References](#)[Tables](#)[Figures](#)[◀](#)[▶](#)[◀](#)[▶](#)[Back](#)[Close](#)[Full Screen / Esc](#)[Printer-friendly Version](#)[Interactive Discussion](#)

Examination of ozonesonde data for trends and trend changes incorporating solar and Arctic oscillation signals, *J. Geophys. Res.*, 111, D13305, doi:10.1029/2005JD006684, 2006.

Nair, P. J., Godin-Beekmann, S., Kuttippurath, J., Ancellet, G., Goutail, F., Pazmiño, A., Froidevaux, L., Zawodny, J. M., Evans, R. D., Wang, H. J., Anderson, J., and Pastel, M.: Ozone trends derived from the total column and vertical profiles at a northern mid-latitude station, *Atmos. Chem. Phys.*, 13, 10373–10384, doi:10.5194/acp-13-10373-2013, 2013.

Neu, J. L., Flury, T., Manney, G. L., Santee, M. L., Livesey, N. J., and Worden, J.: Tropospheric ozone variations governed by changes in stratospheric circulation, *Nat. Geosci.*, 7, 340–344, doi:10.1038/ngeo2138, 2014.

Newchurch, M. J., Yang, E.-S., Cunnold, D. M., Reinsel, G. C., and Zawodny, J. M.: Evidence for slowdown in stratospheric ozone loss: first stage of ozone recovery, *J. Geophys. Res.-Atmos.*, 108, D16, doi:10.1029/2003JD003471, 2003.

Oetjen, H., Payne, V. H., Kulawik, S. S., Eldering, A., Worden, J., Edwards, D. P., Francis, G. L., Worden, H. M., Clerbaux, C., Hadji-Lazaro, J., and Hurtmans, D.: Extending the satellite data record of tropospheric ozone profiles from Aura-TES to MetOp-IASI, *Atmos. Meas. Tech. Discuss.*, 7, 7013–7051, doi:10.5194/amtd-7-7013-2014, 2014.

Oltmans, S. J., Lefohn, A. S., Scheel, H. E., Harris, J. M., Levy I. I., H., Galbally, I. E., Brunke, E., Meyer, C. P., Lathrop, J. A., Johnson, B. J., Shadwick, D. S., Cuevas, E., Schmidlin, F. J., Tarasick, D. W., Claude, H., Kerr, J. B., Uchino, O., and Mohnen, V.: Trends of ozone in the troposphere, *Geophys. Res. Lett.*, 25, 139–142, doi:10.1029/97GL03505, 1998.

Oltmans, S. J., Lefohn, A. S., Harris, J. M., Galbally, I., Scheel, H. E., Bodeker, G., Brunke, E., Claude, H., Tarasick, D., Johnson, B. J., Simmonds, P., Shadwick, D., Anlauf, K., Hayden, K., Schmidlin, F., Fujimoto, T., Akagi, K., Meyer, C., Nichol, S., Davies, J., Redondas, A., and Cuevas, E.: Long-term changes in tropospheric ozone, *Atmos. Environ.*, 40, 3156–3173, 2006.

Parrington, M., Palmer, P. I., Henze, D. K., Tarasick, D. W., Hyer, E. J., Owen, R. C., Helmig, D., Clerbaux, C., Bowman, K. W., Deeter, M. N., Barratt, E. M., Coheur, P.-F., Hurtmans, D., Jiang, Z., George, M., and Worden, J. R.: The influence of boreal biomass burning emissions on the distribution of tropospheric ozone over North America and the North Atlantic during 2010, *Atmos. Chem. Phys.*, 12, 2077–2098, doi:10.5194/acp-12-2077-2012, 2012.

Parrish, D. D., Law, K. S., Staehelin, J., Derwent, R., Cooper, O. R., Tanimoto, H., Volz-Thomas, A., Gilge, S., Scheel, H.-E., Steinbacher, M., and Chan, E.: Long-term changes in

Ozone variability in the troposphere and the stratosphere from the first six years of IASI observations

C. Wespes et al.

Title Page

Abstract

Introduction

Conclusions

References

Tables

Figures

◀

▶

◀

▶

Back

Close

Full Screen / Esc

Printer-friendly Version

Interactive Discussion

lower tropospheric baseline ozone concentrations at northern mid-latitudes, *Atmos. Chem. Phys.*, 12, 11485–11504, doi:10.5194/acp-12-11485-2012, 2012.

Pitts, M. C., Poole, L. R., Dörnbrack, A., and Thomason, L. W.: The 2009–2010 Arctic polar stratospheric cloud season: a CALIPSO perspective, *Atmos. Chem. Phys.*, 11, 2161–2177, doi:10.5194/acp-11-2161-2011, 2011.

Pommier, M., Clerbaux, C., Law, K. S., Ancellet, G., Bernath, P., Coheur, P.-F., Hadji-Lazaro, J., Hurtmans, D., Nédélec, P., Paris, J.-D., Ravetta, F., Ryerson, T. B., Schlager, H., and Weinheimer, A. J.: Analysis of IASI tropospheric O_3 data over the Arctic during POLARCAT campaigns in 2008, *Atmos. Chem. Phys.*, 12, 7371–7389, doi:10.5194/acp-12-7371-2012, 2012.

Randel, W. J. and Wu, F.: Isolation of the ozone QBO in SAGE II data by singular-value decomposition, *J. Atmos. Sci.*, 53, 2546–2559, 1996.

Randel, W. J. and Wu, F.: A stratospheric ozone profile data set for 1979–2005: Variability, trends, and comparisons with column ozone data, *J. Geophys. Res.-Atmos.*, 112, D06313, doi:10.1029/2006JD007339, 2007.

Reinsel, G. C., Weatherhead, E. C., Tiao, G. C., Miller, A. J., Nagatani, R. M., Wuebbles, D. J., and Flynn, L. E.: On detection of turnaround and recovery in trend for ozone, *J. Geophys. Res.*, 107, D10, doi:10.1029/2001JD000500, 2002.

Reinsel, G. C., Miller, A. J., Weatherhead, E. C., Flynn, L. E., Nagatani, R. M., Tiao, G. C., and Wuebbles, D. J.: Trend analysis of total ozone data for turnaround and dynamical contributions, *J. Geophys. Res.*, 110, D16306, doi:10.1029/2004JD004662, 2005.

Rodgers, C. D.: *Inverse Methods for Atmospheric Sounding: Theory and Practice*, Series on Atmospheric, Oceanic and Planetary Physics, Vol. 2, World Scientific Publishing Co., Singapore, 2000.

Rieder, H. E., Frossard, L., Ribatet, M., Staehelin, J., Maeder, J. A., Di Rocco, S., Davison, A. C., Peter, T., Weihs, P., and Holawe, F.: On the relationship between total ozone and atmospheric dynamics and chemistry at mid-latitudes – Part 2: The effects of the El Niño/Southern Oscillation, volcanic eruptions and contributions of atmospheric dynamics and chemistry to long-term total ozone changes, *Atmos. Chem. Phys.*, 13, 165–179, doi:10.5194/acp-13-165-2013, 2013.

Safieddine, S., Clerbaux, C., George, M., Hadji-Lazaro, J., Hurtmans, D., Coheur, P.-F., Wespes, C., Loyola, D., Valks, P., and Hao, N.: Tropospheric ozone and nitrogen dioxide measurements in urban and rural regions as seen by IASI and GOME-2, *J. Geophys. Res.*, 118, 10555–10566, 2013.

Ozone variability in the troposphere and the stratosphere from the first six years of IASI observations

C. Wespes et al.

Title Page

Abstract

Introduction

Conclusions

References

Tables

Figures

◀

▶

◀

▶

Back

Close

Full Screen / Esc

Printer-friendly Version

Interactive Discussion

Salby, M., Callaghan, P., Keckhut, P., Godin, S., and Guirlet, M.: Interannual changes of temperature and ozone: relationship between the lower and upper stratosphere, *J. Geophys. Res.*, 107, 4342, doi:10.1029/2001JD000421, 2002.

Salby, M., Titova, E., and Deschamps, L.: Rebound of Antarctic ozone, *Geophys. Res. Lett.*, 38, L09702, doi:10.1029/2011GL047266, 2011.

Saunois, M., Emmons, L., Lamarque, J.-F., Tilmes, S., Wespes, C., Thouret, V., and Schultz, M.: Impact of sampling frequency in the analysis of tropospheric ozone observations, *Atmos. Chem. Phys.*, 12, 6757–6773, doi:10.5194/acp-12-6757-2012, 2012.

Scannell, C., Hurtmans, D., Boynard, A., Hadji-Lazaro, J., George, M., Delcloo, A., Tuinder, O., Coheur, P.-F., and Clerbaux, C.: Antarctic ozone hole as observed by IASI/MetOp for 2008–2010, *Atmos. Meas. Tech.*, 5, 123–139, doi:10.5194/amt-5-123-2012, 2012.

Schneider, M., Blumenstock, T., Hase, F., Höpfner, M., Cuevas, E., Redondas, A., and Sancho, J. M.: Ozone profiles and total column amounts derived at Izana Tenerife Island, from FTIR solar absorption spectra, and its validation by an intercomparison to ECC-sonde and Brewer spectrometer measurements, *J. Quant. Spectrosc. Ra.*, 91, 245–274, doi:10.1016/j.jqsrt.2004.05.067, 2005.

Shepherd, T. G., Plummer, D. A., Scinocca, J. F., Hegglin, M. I., Fioletov, V. E., Reader, M. C., Remsberg, E., von Clarmann, T., and Wang, H. J.: Reconciliation of halogen-induced ozone loss with the total-column ozone record, *Nat. Geosci.*, 7, 443–449, doi:10.1038/ngeo2155, 2014.

Soukharev, B. E. and Hood, L. L.: Solar cycle variation of stratospheric ozone: multiple regression analysis of long-term satellite data sets and comparisons with models, *J. Geophys. Res.-Atmos.*, 111, D20314, doi:10.1029/2006JD007107, 2006.

Steinbrecht, W., Claude, H., and Winkler, P.: Enhanced upper stratospheric ozone: sign of recovery or solar cycle effect?, *J. Geophys. Res.*, 109, D02308, doi:10.1029/2003JD004284, 2004.

Steinbrecht, W., Claude, H., Schonenborn, F., McDermid, I. S., Leblanc, T., Godin, S., Song, T., Swart, D. P. J., Meijer, Y. J., Bodeker, G. E., Connor, B. J., Kampf, N., Hocke, K., Calisesi, Y., Schneider, N., de la Noe, J., Parrish, A. D., Boyd, I. S., Brühl, C., Steil, B., Giorgetta, M. A., Manzini, E., Thomason, L. W., Zawodny, J. M., McCormick, M. P., Russell III, J. M., Bhatta, P. K., Stolarski, R. S., and Hollandsworth-Friith, S. M.: Long-term evolution of upper stratospheric ozone at selected stations of the network for the detection of stratospheric change (NDSC), *J. Geophys. Res.*, 111, D10308, doi:10.1029/2005JD006454, 2006a.

Ozone variability in the troposphere and the stratosphere from the first six years of IASI observations

C. Wespes et al.

Title Page

Abstract

Introduction

Conclusions

References

Tables

Figures

◀

▶

◀

▶

Back

Close

Full Screen / Esc

Printer-friendly Version

Interactive Discussion

Steinbrecht, W., Haßler, B., Brühl, C., Dameris, M., Giorgetta, M. A., Grewe, V., Manzini, E., Matthes, S., Schnadt, C., Steil, B., and Winkler, P.: Interannual variation patterns of total ozone and lower stratospheric temperature in observations and model simulations, *Atmos. Chem. Phys.*, 6, 349–374, doi:10.5194/acp-6-349-2006, 2006b.

Steinbrecht, W., Claude, H., Schöenborn, F., McDermid, I. S., Leblanc, T., Godin-Beekmann, S., Keckhut, P., Hauchecorne, A., Van Gijssel, J. A. E., Swart, D. P. J., Bodeker, G. E., Parrish, A., Boyd, I. S., Kämpfer, N., Hocke, K., Stolarski, R. S., Frith, S. M., Thomason, L. W., Remsberg, E. E., Von Savigny, C., Rozanov, A., and Burrows, J. P.: Ozone and temperature trends in the upper stratosphere at five stations of the network for the detection of atmospheric composition change, *Int. J. Remote Sens.*, 30, 3875–3886, doi:10.1080/01431160902821841, 2009.

Stolarski, R. S. and Frith, S. M.: Search for evidence of trend slow-down in the long-term TOMS/SBUV total ozone data record: the importance of instrument drift uncertainty, *Atmos. Chem. Phys.*, 6, 4057–4065, doi:10.5194/acp-6-4057-2006, 2006.

Tian, W., Chipperfield, M. P., Gray, L. J., and Zawodny, J. M.: Quasi-biennial oscillation and tracer distributions in a coupled chemistry-climate model, *J. Geophys. Res.*, 111, D20301, doi:10.1029/2005JD006871, 2006.

Varai, A., Homonnai, V., Jánosi, I. M., and Müller, R.: Early signatures of ozone trend reversal over the Antarctic, *Earth's Future*, 3, 95–109, doi:10.1002/2014EF000270, 2015.

Vigouroux, C., De Mazière, M., Demoulin, P., Servais, C., Hase, F., Blumenstock, T., Kramer, I., Schneider, M., Mellqvist, J., Strandberg, A., Velasco, V., Notholt, J., Sussmann, R., Stremme, W., Rockmann, A., Gardiner, T., Coleman, M., and Woods, P.: Evaluation of tropospheric and stratospheric ozone trends over Western Europe from ground-based FTIR network observations, *Atmos. Chem. Phys.*, 8, 6865–6886, doi:10.5194/acp-8-6865-2008, 2008.

Vigouroux, C., Blumenstock, T., Coffey, M., Errera, Q., García, O., Jones, N. B., Hannigan, J. W., Hase, F., Liley, B., Mahieu, E., Mellqvist, J., Notholt, J., Palm, M., Persson, G., Schneider, M., Servais, C., Smale, D., Thölix, L., and De Mazière, M.: Trends of ozone total columns and vertical distribution from FTIR observations at 8 NDACC stations around the globe, *Atmos. Chem. Phys. Discuss.*, 14, 24623–24666, doi:10.5194/acpd-14-24623-2014, 2014.

Weatherhead, E. C. and Andersen, S. B.: The search for signs of recovery of the ozone layer, *Nature*, 441, 39–45, doi:10.1038/nature04746, 2006.

Ozone variability in the troposphere and the stratosphere from the first six years of IASI observations

C. Wespes et al.

Title Page

Abstract

Introduction

Conclusions

References

Tables

Figures

◀

▶

◀

▶

Back

Close

Full Screen / Esc

Printer-friendly Version

Interactive Discussion



Weiss, A. K., Staehelin, J., Appenzeller, C., and Harris, N. R. P.: Chemical and dynamical contributions to ozone profile trends of the Payerne (Switzerland) balloon soundings, *J. Geophys. Res.*, 106, 22685–22694, 2001.

Wespes, C., Hurtmans, D., Clerbaux, C., Santee, M. L., Martin, R. V., and Coheur, P. F.: Global distributions of nitric acid from IASI/MetOP measurements, *Atmos. Chem. Phys.*, 9, 7949–7962, doi:10.5194/acp-9-7949-2009, 2009.

Wespes, C., Emmons, L., Edwards, D. P., Hannigan, J., Hurtmans, D., Saunio, M., Coheur, P. F., Clerbaux, C., Coffey, M. T., Batchelor, R. L., Lindenmaier, R., Strong, K., Weinheimer, A. J., Nowak, J. B., Ryerson, T. B., Crounse, J. D., and Wennberg, P. O.: Analysis of ozone and nitric acid in spring and summer Arctic pollution using aircraft, ground-based, satellite observations and MOZART-4 model: source attribution and partitioning, *Atmos. Chem. Phys.*, 12, 237–259, doi:10.5194/acp-12-237-2012, 2012.

WMO: Scientific Assessment of Ozone Depletion: 2002, Global Ozone Research and Monitoring Project – Report No. 47, World Meteorological Organization, Geneva, Switzerland, 2003.

WMO: Scientific Assessment of Ozone Depletion: 2006, Global Ozone Research and Monitoring Project – Report 50, World Meteorological Organization, Geneva, Switzerland, 2007.

WMO: Scientific Assessment of Ozone Depletion: 2010, Global Ozone Research and Monitoring Project – Report 52, World Meteorological Organization, Geneva, Switzerland, 2011.

WMO: Scientific Assessment of Ozone Depletion: 2014, Global Ozone Research and Monitoring Project – Report 56, World Meteorological Organization, Geneva, Switzerland, 2014.

Yang, E.-S., Cunnold, D. M., Salawitch, R. J., McCormick, M. P., Russell, J., Zawodny, J. M., Oltmans, S., and Newchurch, M. J.: Attribution of recovery in lower-stratospheric ozone, *J. Geophys. Res.*, 111, D17309, doi:10.1029/2005JD006371, 2006.

Ozone variability in the troposphere and the stratosphere from the first six years of IASI observations

C. Wespes et al.

Title Page

Abstract

Introduction

Conclusions

References

Tables

Figures

◀

▶

◀

▶

Back

Close

Full Screen / Esc

Printer-friendly Version

Interactive Discussion

Table 1. List of the proxies used in this study and their sources.

Proxy	Description (resolution)	Sources
F10.7	The 10.7 cm solar radio flux (daily or monthly)	NOAA National Weather Service Climate Prediction Center: ftp://ftp.ngdc.noaa.gov/STP/space-weather/solar-data/solar-features/solar-radio/noontime-flux/penticton/penticton_adjusted/listings/listing_drao_noontime-flux-adjusted_daily.txt or ftp://ftp.ngdc.noaa.gov/STP/space-weather/solar-data/solar-features/solar-radio/noontime-flux/penticton/penticton_adjusted/listings/listing_drao_noontime-flux-adjusted_monthly.txt
QBO ¹⁰ QBO ³⁰	Quasi-Biennial Oscillation index at 10 and 30 hPa (monthly)	Free University of Berlin: www.geo.fu-berlin.de/en/met/ag/strat/produkte/qbo/
ENSO	El Niño/Southern Oscillation – Nino 3.4 Index (3 monthly averages)	NOAA National Weather Service Climate Prediction Center: http://www.cpc.noaa.gov/data/indices/
NAO	North Atlantic Oscillation index (daily or monthly)	ftp://ftp.cpc.ncep.noaa.gov/cwlinks/norm.daily.nao.index.b500101.current.ascii or http://www.cpc.ncep.noaa.gov/products/precip/CWlink/pna/norm.nao.monthly.b5001.current.ascii
AAO	Antarctic Oscillation index (daily or monthly)	ftp://ftp.cpc.ncep.noaa.gov/cwlinks/norm.daily.aao.index.b790101.current.ascii or http://www.cpc.ncep.noaa.gov/products/precip/CWlink/daily_ao_index/aao/monthly.aao.index.b79.current.ascii

Ozone variability in the troposphere and the stratosphere from the first six years of IASI observations

C. Wespes et al.

Table 3. Same as Table 2 but for seasonal O₃ trends and associated uncertainties based on daily medians during JJA (top row) and DJF (bottom row) periods. Values marked with a star (*) refers to trends which are rejected by the iterative backward elimination procedure^a.

DUyr ⁻¹	# Days	Ground–300 hPa (Troposphere)	300–150 hPa (UTLS)	150–25 hPa (MLS)	25–3 hPa (US)	Total columns
70–90° N (Feb–Oct)	613 48	-0.18 ± 0.08 –	1.13 ± 0.65 –	-0.91 ± 1.52 –	1.72 ± 0.51 –	1.36 ± 1.15 –
50–70° N	551 527	-0.23 ± 0.07 -0.09 ± 0.12*	1.03 ± 0.37 1.74 ± 1.30	0.62 ± 1.64 0.73 ± 1.73*	1.67 ± 0.48 -0.66 ± 0.79	3.01 ± 1.64 1.56 ± 2.66*
30–50° N	551 529	-0.30 ± 0.10 -0.24 ± 0.09	0.42 ± 0.30 0.28 ± 0.28	-0.30 ± 0.65* -0.82 ± 0.90	0.84 ± 0.25 0.62 ± 0.49	1.17 ± 1.35 -0.81 ± 1.05
10–30° N	551 529	-0.05 ± 0.16* 0.18 ± 0.14	0.17 ± 0.05 0.01 ± 0.09*	-0.34 ± 0.30 -1.05 ± 0.45	0.36 ± 0.27 0.49 ± 0.54*	-0.09 ± 0.54* -1.14 ± 0.44
10° S–10° N	551 529	-0.06 ± 0.10 -0.70 ± 0.23	0.04 ± 0.05* -0.32 ± 0.10	-0.84 ± 0.86 1.64 ± 1.77	0.32 ± 0.42 0.53 ± 0.59	-0.56 ± 0.74 0.34 ± 0.93*
30–10° S	551 530	-0.26 ± 0.09 -0.15 ± 0.11	-0.06 ± 0.07 0.06 ± 0.12*	-0.56 ± 0.40 -0.12 ± 0.31*	1.06 ± 0.55 1.48 ± 0.53	0.24 ± 0.43 1.56 ± 0.92
50–30° S	551 529	-0.21 ± 0.05 -0.10 ± 0.06	-0.16 ± 0.09 -0.14 ± 0.06	-0.52 ± 0.54 -2.83 ± 0.64	0.49 ± 0.59 3.40 ± 0.85	-0.44 ± 0.83 0.47 ± 0.52
70–50° S	551 529	-0.25 ± 0.06 -0.10 ± 0.04	1.03 ± 0.60 0.19 ± 0.24*	2.63 ± 1.65 0.52 ± 0.48	0.98 ± 0.62 1.66 ± 0.70	3.44 ± 2.47 1.72 ± 0.74
90–70° S (Oct–Apr)	– 523	– -0.21 ± 0.20	– -0.46 ± 0.80*	– 0.16 ± 2.53*	– 1.18 ± 0.67	– 0.98 ± 3.27*

^a The trend values result from the adjustment of the regression model where the linear term is kept whatever its *p* value calculated during the iterative process.

Title Page

Abstract

Introduction

Conclusions

References

Tables

Figures

◀

▶

◀

▶

Back

Close

Full Screen / Esc

Printer-friendly Version

Interactive Discussion

Ozone variability in the troposphere and the stratosphere from the first six years of IASI observations

C. Wespes et al.

Title Page

Abstract

Introduction

Conclusions

References

Tables

Figures

◀

▶

◀

▶

Back

Close

Full Screen / Esc

Printer-friendly Version

Interactive Discussion



Table 4. Ozone trends and associated uncertainties (95 % confidence limits), given in DU yr^{-1} over NDACC (Network for the Detection of Atmospheric Composition Change) stations in the N.H. based on daily medians of IASI (within a grid box of $1^\circ \times 1^\circ$ centered on stations, top row) and FTIR observations (successive rows for different time intervals). Bold values refer to statistically significant trends. Values marked with a star (*) refers to trends which are rejected by the iterative backward elimination procedure^a.

DU yr^{-1}	Data periods	# days	25–3 hPa (US)	Total columns
Ny-Alesund (79° N)	2008–2013	1239	0.56 ± 0.73	5.26 ± 4.72
	2008–2012	84	-3.58 ± 4.58	$2.24 \pm 20.78^*$
	2003–2012	168	$-0.17 \pm 0.70^*$	-4.84 ± 3.01
	2000–2012	288	0.64 ± 0.60	$-1.02 \pm 2.40^*$
	1999–2012	320	0.62 ± 0.55	-2.35 ± 1.40
	1995–2012	383	1.03 ± 0.66	$1.31 \pm 2.39^*$
Thule (77° N)	1995–2003	167	1.25 ± 1.05	3.33 ± 3.41
	2008–2013	1094	1.24 ± 1.09	4.97 ± 4.72
	2008–2012	340	-2.10 ± 2.89	$0.39 \pm 11.59^*$
	2003–2012	697	0.86 ± 0.89	-2.77 ± 2.99
	2000–2012	776	1.33 ± 0.86	-1.29 ± 1.73
	1999–2012	779	1.69 ± 0.88	-1.25 ± 1.74
Kiruna (68° N)	1999–2003	138	3.73 ± 2.90	$4.86 \pm 10.13^*$
	2008–2013	1236	$0.21 \pm 1.42^*$	4.41 ± 4.00
	2008–2012	254	$-1.97 \pm 6.04^*$	$-3.75 \pm 6.64^*$
	2003–2012	678	$0.15 \pm 0.67^*$	2.26 ± 3.68
	2000–2012	913	1.60 ± 1.29	3.69 ± 4.20
	1999–2012	984	1.10 ± 0.98	$-0.43 \pm 1.64^*$
Jungfraujoch (47° N)	1996–2012	1183	1.11 ± 0.54	1.82 ± 1.77
	1996–2003	596	1.26 ± 1.21	$1.12 \pm 3.77^*$
	2008–2013	1580	2.95 ± 0.61	5.64 ± 3.15
	2008–2012	565	1.60 ± 1.80	5.28 ± 4.82
	1998–2012	1582	0.10 ± 0.35	$-0.28 \pm 0.86^*$
	1995–2012	1771	$0.02 \pm 0.33^*$	0.85 ± 0.79
Zugspitze (47° N)	2008–2013	1729	3.17 ± 0.56	5.53 ± 2.92
	2008–2012	597	0.71 ± 1.22	3.46 ± 3.79
	1998–2012	1472	$0.08 \pm 0.32^*$	0.81 ± 0.98
	1995–2012	1525	0.23 ± 0.32	1.36 ± 1.01
Izana (28° N)	2008–2013	1803	0.56 ± 0.65	1.28 ± 0.77
	2008–2012	443	$0.24 \pm 0.80^*$	$0.91 \pm 2.44^*$
	1999–2012	1257	0.46 ± 0.25	$0.20 \pm 0.33^*$

^a The trend values result from the adjustment of the regression model where the linear term is kept whatever its p value calculated during the iterative process.

Ozone variability in the troposphere and the stratosphere from the first six years of IASI observations

C. Wespes et al.

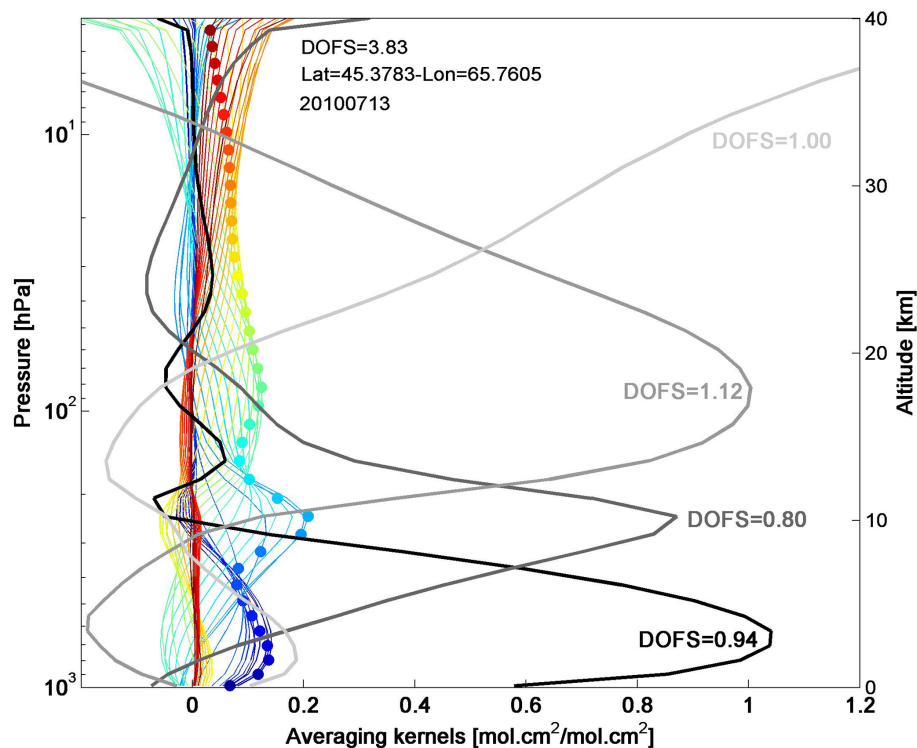


Figure 1. Typical IASI FORLI-O₃ averaging kernels, in partial column units, corresponding to one mid-latitude observation in July (45° N/66° E) for each 1 km retrieved layers from ground to 40 km altitude (color scale) and for 4 merged layers: ground–300; 300–150; 150–25; 25–3 hPa (grey lines). The total DOFS and the DOFS for each merged layers are also indicated.

Title Page

Abstract

Introduction

Conclusions

References

Tables

Figures

◀

▶

◀

▶

Back

Close

Full Screen / Esc

Printer-friendly Version

Interactive Discussion

Ozone variability in the troposphere and the stratosphere from the first six years of IASI observations

C. Wespes et al.

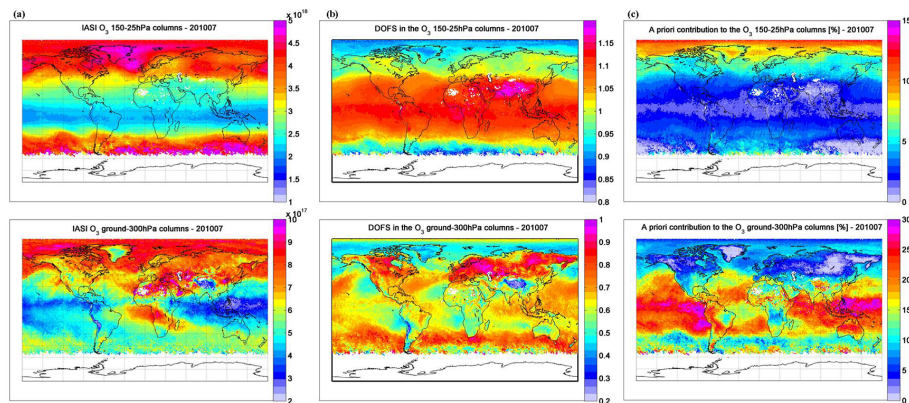


Figure 2. Distributions of (a) O₃ columns, (b) DOFS and (c) a priori contribution (given as a %) in the ground–300 and 150–25 hPa layers for IASI O₃, averaged over July 2010 daytime data. Note that the scales are different.

Title Page

Abstract

Introduction

Conclusions

References

Tables

Figures

◀

▶

◀

▶

Back

Close

Full Screen / Esc

Printer-friendly Version

Interactive Discussion

Ozone variability in the troposphere and the stratosphere from the first six years of IASI observations

C. Wespes et al.

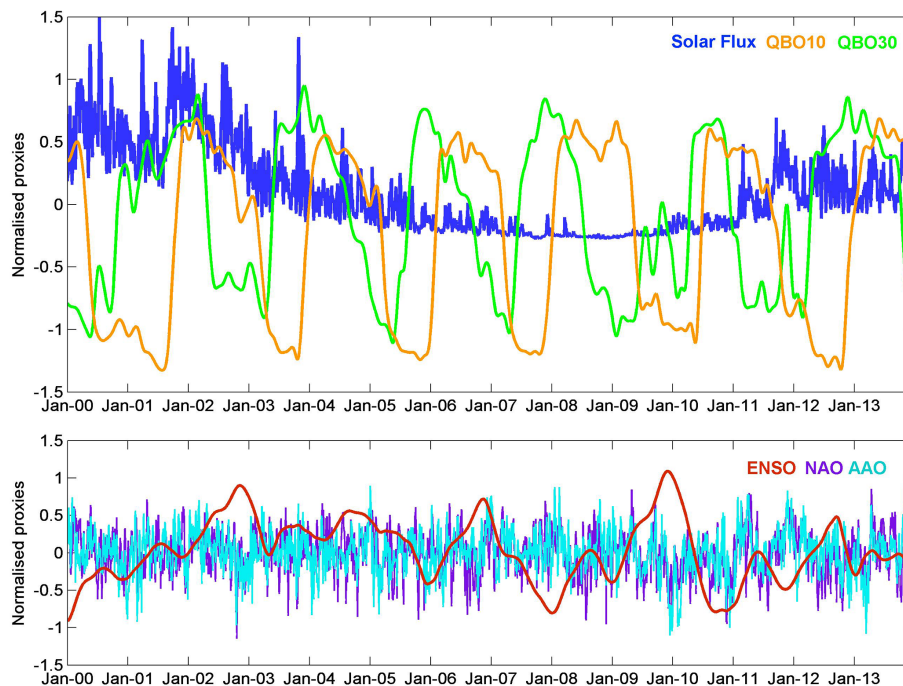


Figure 3. Normalized proxies as a function of time for the period 2000–2013 for the solar F10.7 cm radio flux (blue) and the equatorial winds at 10 (green) and 30 hPa (orange), respectively (top panel), and for the El Niño (red), north Atlantic oscillation (purple) and Antarctic oscillation (light blue) indexes (bottom panel).

Ozone variability in the troposphere and the stratosphere from the first six years of IASI observations

C. Wespes et al.

Title Page

Abstract

Introduction

Conclusions

References

Tables

Figures

◀

▶

◀

▶

Back

Close

Full Screen / Esc

Printer-friendly Version

Interactive Discussion

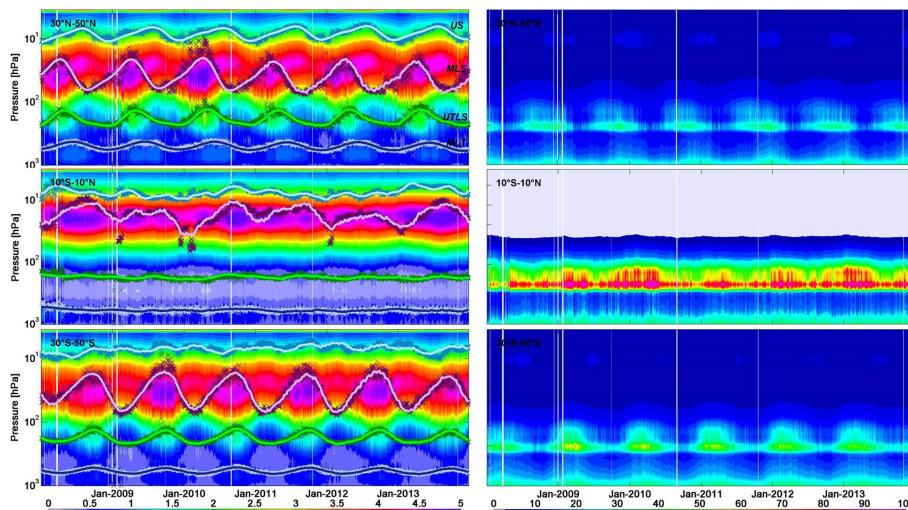


Figure 4. (a) Daily IASI O₃ profiles (1×10^{12} molecules cm^{-3}) for the period 2008–2013 and over the range of the retrieved profiles as a function of time and altitude, in three latitude bands: 30–50° N (top), 10° S–10° N (middle), 30–50° S (bottom). Superimposed daily IASI O₃ partial columns (scatters) and the associated fits (solid lines) from the multivariate regressions for the MLT (ground–300 hPa), UTLS (300–150 hPa), MLS (150–25 hPa) and US (above 25 hPa) layers. The IASI measurements and the fits have been scaled for clarity. (b) Estimated total retrieval errors (%) associated with daily IASI O₃ profiles.

Ozone variability in the troposphere and the stratosphere from the first six years of IASI observations

C. Wespes et al.

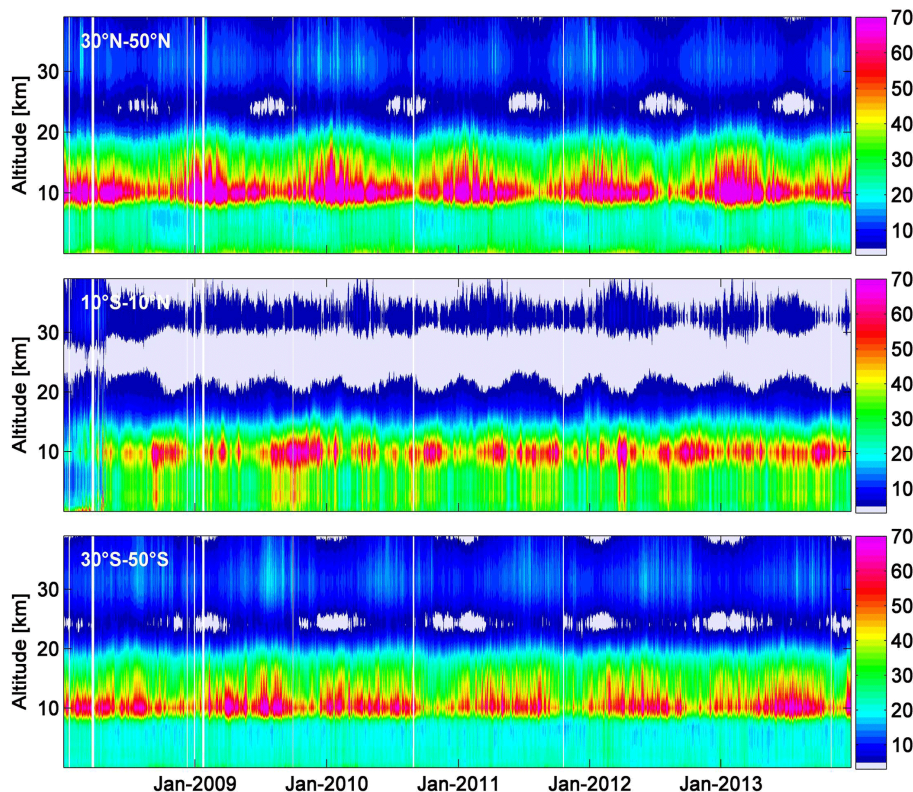


Figure 5. Daily IASI O₃ variability (%), expressed as $1 \times \sigma$ relative to the median values, where σ is the standard deviation, as a function of time and altitude in three latitude bands: 30–50° N (top), 10° S–10° N (middle), 30–50° S (bottom).

Ozone variability in the troposphere and the stratosphere from the first six years of IASI observations

C. Wespes et al.

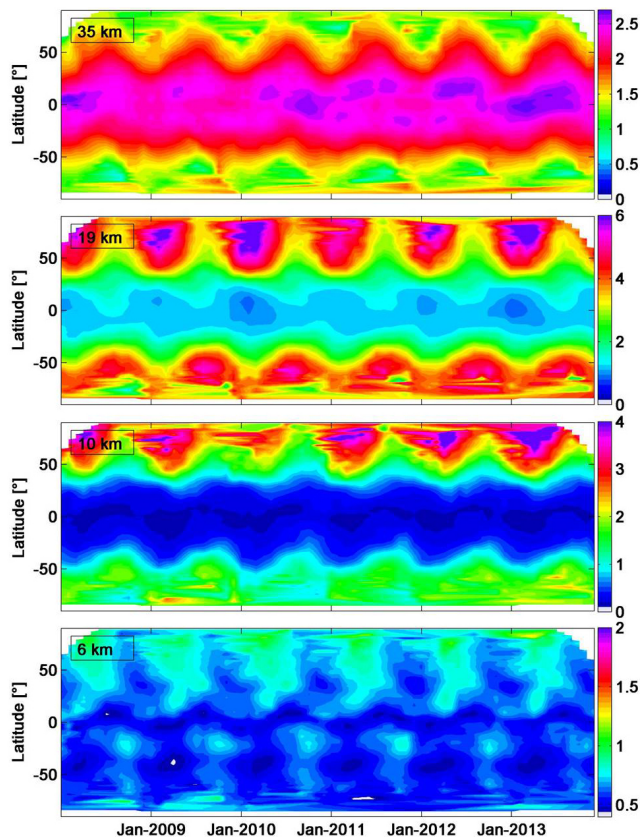


Figure 6. Daily IASI O₃ number density (1×10^{12} molecules cm⁻³) at 35 km (top), 19 km (middle), 10 km (middle) and 6 km (bottom) as a function of time and latitude. Note that the color scales are different.

[Title Page](#)[Abstract](#)[Introduction](#)[Conclusions](#)[References](#)[Tables](#)[Figures](#)[◀](#)[▶](#)[◀](#)[▶](#)[Back](#)[Close](#)[Full Screen / Esc](#)[Printer-friendly Version](#)[Interactive Discussion](#)

Ozone variability in the troposphere and the stratosphere from the first six years of IASI observations

C. Wespes et al.

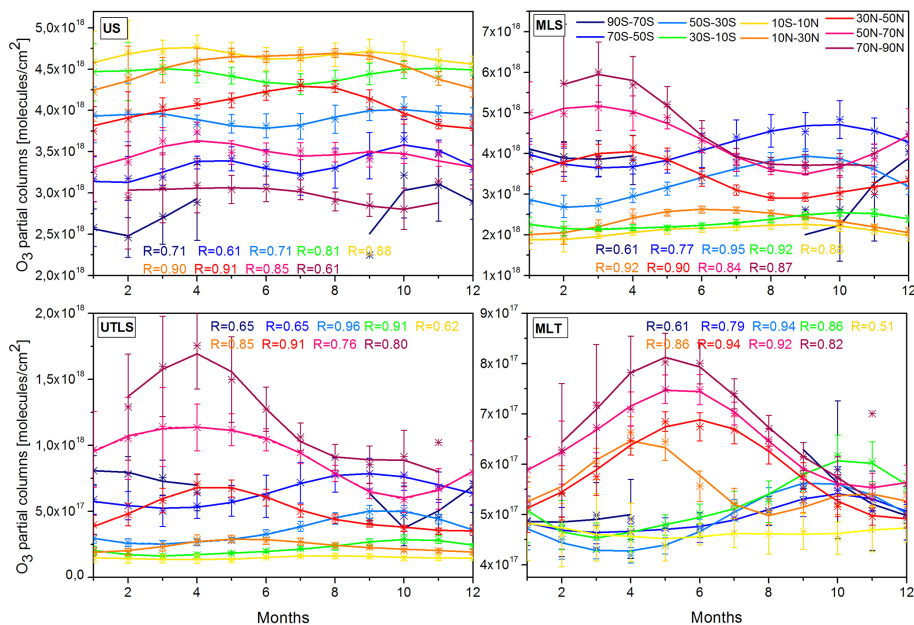


Figure 7. Monthly medians of measured (scatters) and of fitted (line) IASI O₃ columns averaged over the period 2008–2013, for the US, MLS, UTLS and MLT layers and for each 20° latitude bands (color scale). The fit is based on daily medians. Error bars give the 1σ standard deviation relative to the monthly median values. Correlation coefficient (R) between the daily median observations and the fit are also indicated. Note that the scales are also different.

Title Page

Abstract

Introduction

Conclusions

References

Tables

Figures

◀

▶

◀

▶

Back

Close

Full Screen / Esc

Printer-friendly Version

Interactive Discussion

Ozone variability in the troposphere and the stratosphere from the first six years of IASI observations

C. Wespes et al.

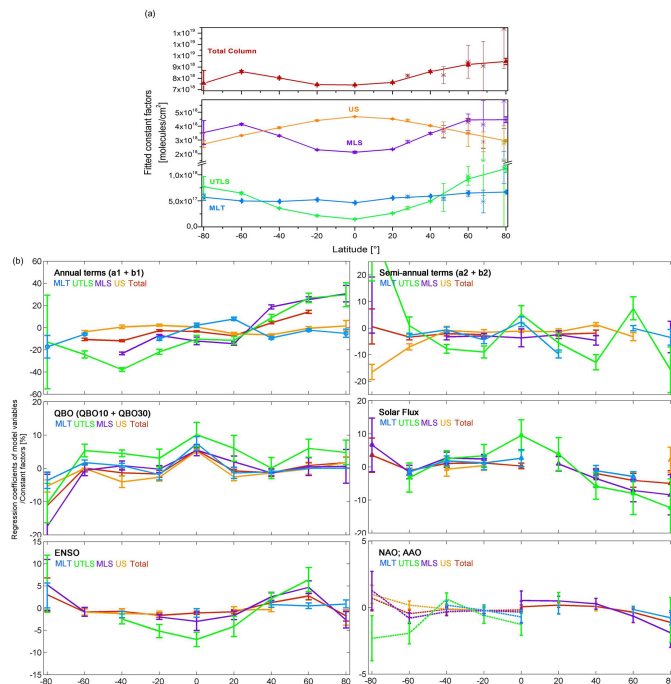


Figure 8. (a) Fitted constant factors (Cst, see Eq. (1), Sect. 3) from the 6 years IASI daily O₃ time series for the 20° latitude belts, separately given for the 4 layers and for the total column. The stars correspond to the constant factors fitted above ground-based measurement stations: Ny-Ålesund (79° N), Kiruna (68° N), Harestua (60° N), Jungfraujoch (47° N), Izana (28° N). (b) Regression coefficients of the variables retained by the stepwise procedure, given in % as $[(\text{regression_coefficients})/\text{fitted_Cst}] \times 100\%$. Identification for the variables: annual (top left) and Semi-Annual variations (top right) terms, QBO at 10 and 30 hPa (bottom left), solar flux (bottom right). Note that the scales are different. The associated fitting uncertainties (95% confidence limits) are also represented (error bars).

Ozone variability in the troposphere and the stratosphere from the first six years of IASI observations

C. Wespes et al.

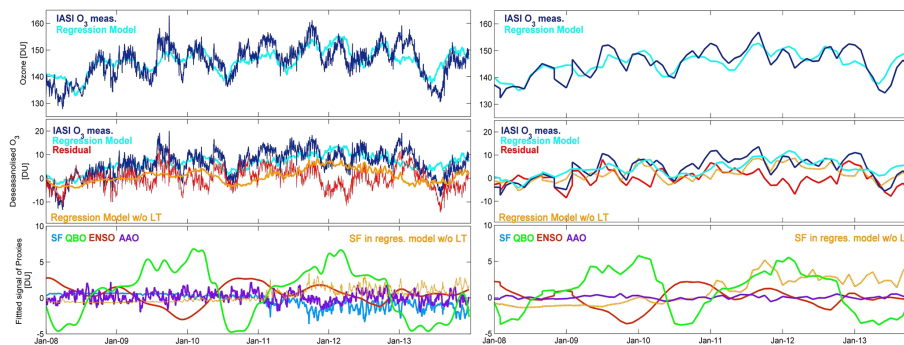


Figure 9. Daily **(a)** and monthly **(b)** time series of O_3 measurements and of the fitted regression model in the US in the $30\text{--}50^\circ$ S latitude band (top), of the deseasonalised O_3 (middle), and of the fitted signal of proxies ([regression coefficients*Proxy]): SF (blue), QBO ($QBO^{10} + QBO^{30}$; green), ENSO (red) and AAO (purple) (given in DU) (bottom).

Title Page

Abstract

Introduction

Conclusions

References

Tables

Figures

◀

▶

◀

▶

Back

Close

Full Screen / Esc

Printer-friendly Version

Interactive Discussion

Ozone variability in the troposphere and the stratosphere from the first six years of IASI observations

C. Wespes et al.

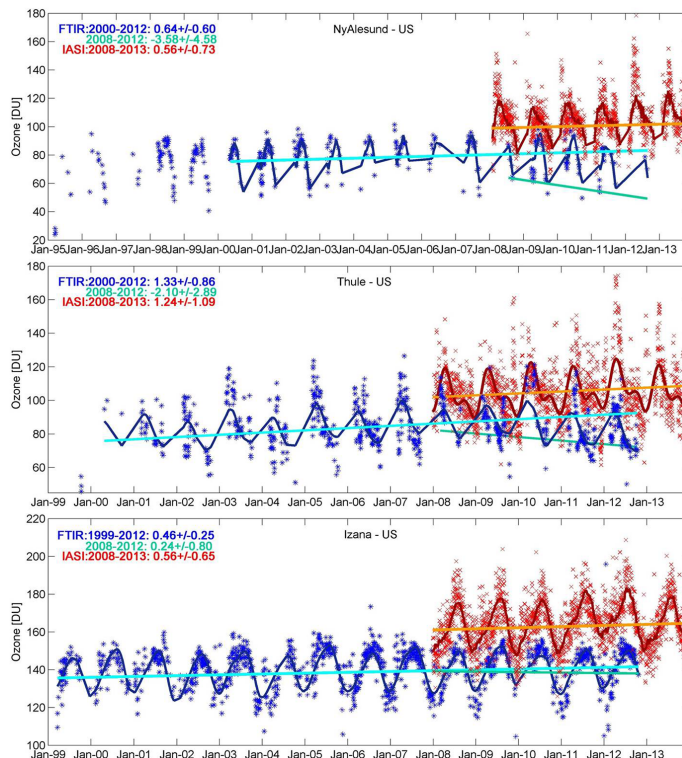


Figure 10. Daily time series of O_3 FTIR (blue symbols) and IASI (red symbols) measurements in the US at Ny-Alesund (top), Thule (middle) and Izana (bottom), covering the 1995–2012 and the 1999–2012 periods, respectively (given in DU). The fitted regression models (dark blue and dark red lines, for FTIR and IASI, respectively) and the linear trends calculated for periods starting after the turnaround over 1999/2000–2012 and over 2008–2012 for FTIR (light blue and green lines), and the 2008–2013 period for IASI (orange line) are also represented ($DU yr^{-1}$). The trend values given in $DU yr^{-1}$ are indicated.